Spatial distribution of particulate matter on winter nights in Temuco, Chile: studying the impact of residential wood-burning using mobile monitoring

Estela Blanco[a], Francisco Rubilar[b], Maria Elisa Quinteros[c], Karen Cayupi[b], Salvador Ayala[a], Siyao Lu[d], Raquel B. Jimenez[e], Juan Pablo Cárdenas[b], Carola A. Blazquez[f], Juana Maria Delgado-Saborit[g,h], Roy M. Harrison[g,i], Pablo Ruiz-Rudolph[j*]

[a] Programa de Doctorado en Salud Pública, Instituto de Salud Poblacional, Facultad de Medicina, Universidad de Chile, Independencia 939, Independencia, Santiago, Chile.
[b] Instituto del Medio Ambiente, Universidad de La Frontera, Avenida Francisco Salazar 01145, Temuco, Chile.
[c] Departamento de Salud Pública. Facultad de Ciencias de la Salud, Universidad de Talca, Avenida Lircay s/n, Talca, Chile.
[d] Department of Environmental Health Sciences, University of Michigan, 1415 Washington Heights, Ann Arbor, MI 48109, USA.
[e] Department of Environmental Health, School of Public Health, Boston University, Boston, MA, USA
[f] Department of Engineering Sciences, Universidad Andres Bello, Quillota 980, Viña del Mar, 2531015, Chile.
[g] Division of Environmental Health and Risk Management, School of Geography, Earth and Environmental Sciences, University of Birmingham, Birmingham, UK.
[h] Perinatal Epidemiology, Environmental Health and Clinical Research, School of Medicine, Universitat Jaume I, Avinguda de Vicent Sos Baynat, s/n, 12071 Castelló de la Plana, Castellon, Spain.
[i] Department of Environmental Sciences / Center of Excellence in Environmental Studies, King Abdulaziz University, PO Box 80203, Jeddah, 21589, Saudi Arabia.
[j] Programa de Salud Ambiental, Instituto de Salud Poblacional, Facultad de Medicina, Universidad de Chile, Independencia 939, Independencia, Santiago, Chile.
[*]Corresponding author

Corresponding Author
Pablo Ruiz-Rudolph. Programa de Salud Ambiental, Instituto de Salud Poblacional, Facultad de Medicina, Universidad de Chile, Independencia 939, Independencia, Santiago, Chile; pabloruizr@uchile.cl; phone (+56-22-978-6379)

Abstract

Temuco, a medium-sized city in the south of Chile, is heavily impacted by residential wood-burning particularly in winter, which causes strong episodes of air pollution. We spatially characterized the distribution of particulate matter (PM) during winter nights in Temuco using mobile measurements. In winter 2016 (June 8-July 15th), continuous monitors for PM ≤ 2.5 μm ($PM_{2.5}$) and ultrafine particles <0.1 μm (UFP) were deployed in a vehicle along with a positioning system during 20 nights (20:00 to 2:00) in assigned routes that crossed the city and additional sampling was conducted at a central site. Measurements were expressed as concentrations and ratios to central site concentrations and collapsed by spatial grids of 50, 100, 200, and 400 meters. Average $PM_{2.5}$ concentrations were ~100 μg m^{-3}, while UFP ~30,000 counts cm^{-3}. Some neighborhoods had concentrations of $PM_{2.5}$ nearly double those measured at a centrally located site, while other neighborhoods had less than half the measured level. We identified hotspots and cold spots of $PM_{2.5}$ and UFP throughout the urban area—and observed some neighborhoods in which over 20 % of the area was categorized as a hotspot for one of the pollutants (14 for $PM_{2.5}$ and 11 for UFP out of 34). Using mobile monitoring—a relatively simple and inexpensive methodology— we characterized the spatial distribution of pollutants and likely clusters for the time period, which may guide future spatial campaigns and help targeting local interventions aimed at air pollution mitigation.

Keywords: air pollution; air quality; wood smoke; global positioning system; mobile sampling

Graphical Abstract

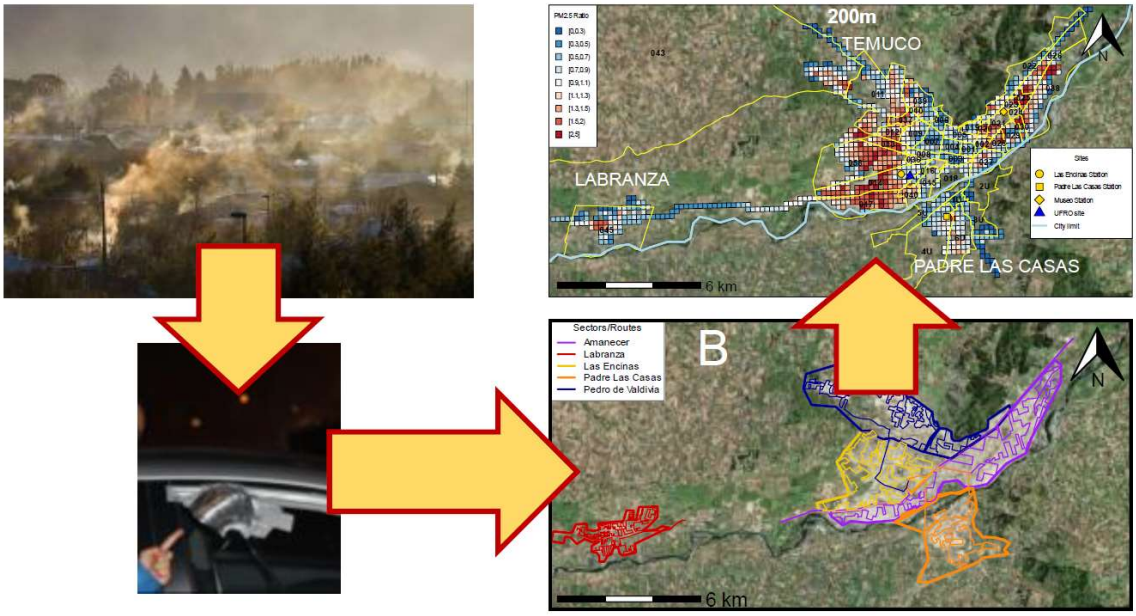

List of tables

List of figures

Supplementary Material

1. Introduction

Wood-burning is a primary energy source for heating throughout the world. It is often less expensive that other energy sources, and in many places populations show a cultural preference (1). Additionally, it is renewable (2), thus it has been occasionally encouraged as a means of mitigating the effects of climate change and energy insecurity (3,4). However, due to inefficient combustion, residential wood-burning is also a large source of air pollutants, including particulate matter (PM) and carbon monoxide (CO), in addition to known human carcinogens, such as benzene and polycyclic aromatic hydrocarbons, which in turn have been linked to negative health outcomes (5).

Residential wood-burning is widespread in Chile, particularly in cities south of the capital, with massive emissions that have led to a large air pollution problem (6), in contrast to northern and central Chilean cities where other sources dominate (7–10). Thus, in cold, winter days, most southern Chilean cities present large episodes of air pollution, exceeding national regulations and affecting public health (11,12). In Temuco, 90% of PM emissions are attributed to household use of wood for heating (13) due to its lower price (14,15).

Adequately monitoring an air pollution problem, such as the one generated by residential wood-burning, requires an air pollution management system, which usually depends on stationary air monitoring that provides real-time information and evaluates the effectiveness of reduction efforts over time. However, stationary systems often mask intra-urban spatial variability, such as hotspots (e.g., areas of particular high levels of air pollution) (16) or spatial gradients (17), which result from the interactions between emission sources, geography, and meteorological factors (18). As an alternative, mobile

129 air quality monitoring has emerged as an economical and fast solution, providing spatial
130 and temporal resolution to the air pollution problem (19).

131 Mobile measurement have been performed by pedestrians (16), persons using
132 public transportation (20), bicycles (20–22) and motorized vehicles (23–26). Most often,
133 monitoring had been performed following predetermined routes to map air pollution in
134 particular zones (20,27,28). Depending on the local context, mobile measurements may
135 focus on different air pollutants, for instance CO, PM ≤ 2.5 μm ($PM_{2.5}$) and ultrafine
136 particles <0.1 μm (UFP) when studying traffic emissions (20,29) or PM for wood-burning
137 (30) or for identification of hotspots of contaminant concentrations (16,19).

138 For the case of urban areas impacted by residential wood-burning, a limited amount
139 of mobile monitoring studies have been conducted (23,25,26,31–36). Studies have mostly
140 been conducted in Canada, the United States, and parts of Europe, mainly in rural or non-
141 urban settings, with relatively low levels of wood-smoke pollution, yet have demonstrated
142 spatial variability and identified hotspots. Many cities around the world are struggling to
143 effectively mitigate the extremely high levels of ambient air pollution as a result of
144 residential wood-burning (37,38). Identifying spatial gradients and local hotspots in highly
145 polluted cities might serve to design better health studies and target measures to improve
146 air quality, particularly for vulnerable populations around hotspots. With this aim, we
147 conducted a mobile measurement campaign to spatially characterize the distribution of
148 PM during winter nights in Temuco, a mid-size city in southern Chile that is heavily
149 impacted by residential wood-burning.
150

2. Material and methods

2.1 Study design and site

We conducted a mobile monitoring field campaign during 20 nights in the urban area of Temuco, Chile, the time of the day with the largest residential wood-burning impact (39). Temuco is located in a valley surrounded by hills and is the conurbation of two neighbor municipalities, Temuco and Padre Las Casas (Figure 1 A), which are separated by the Cautín river in the Araucanía region of Chile. Labranza, a satellite town, is located 13 kilometers west of Temuco. The three cities have a combined population of 358,541 inhabitants (40). Samplers were deployed in vehicles, with the inlet fixed outside the side window, in order to sample continuously across five predetermined routes covering the entire urban area (Figure 1 B). Two fractions of PM were monitored: $PM_{2.5}$ and UFP, as the former is well associated with wood-burning emissions (peak size distribution between 0.25 and 0.4 μm) (5,41,42), while the latter mostly with traffic emissions (43).

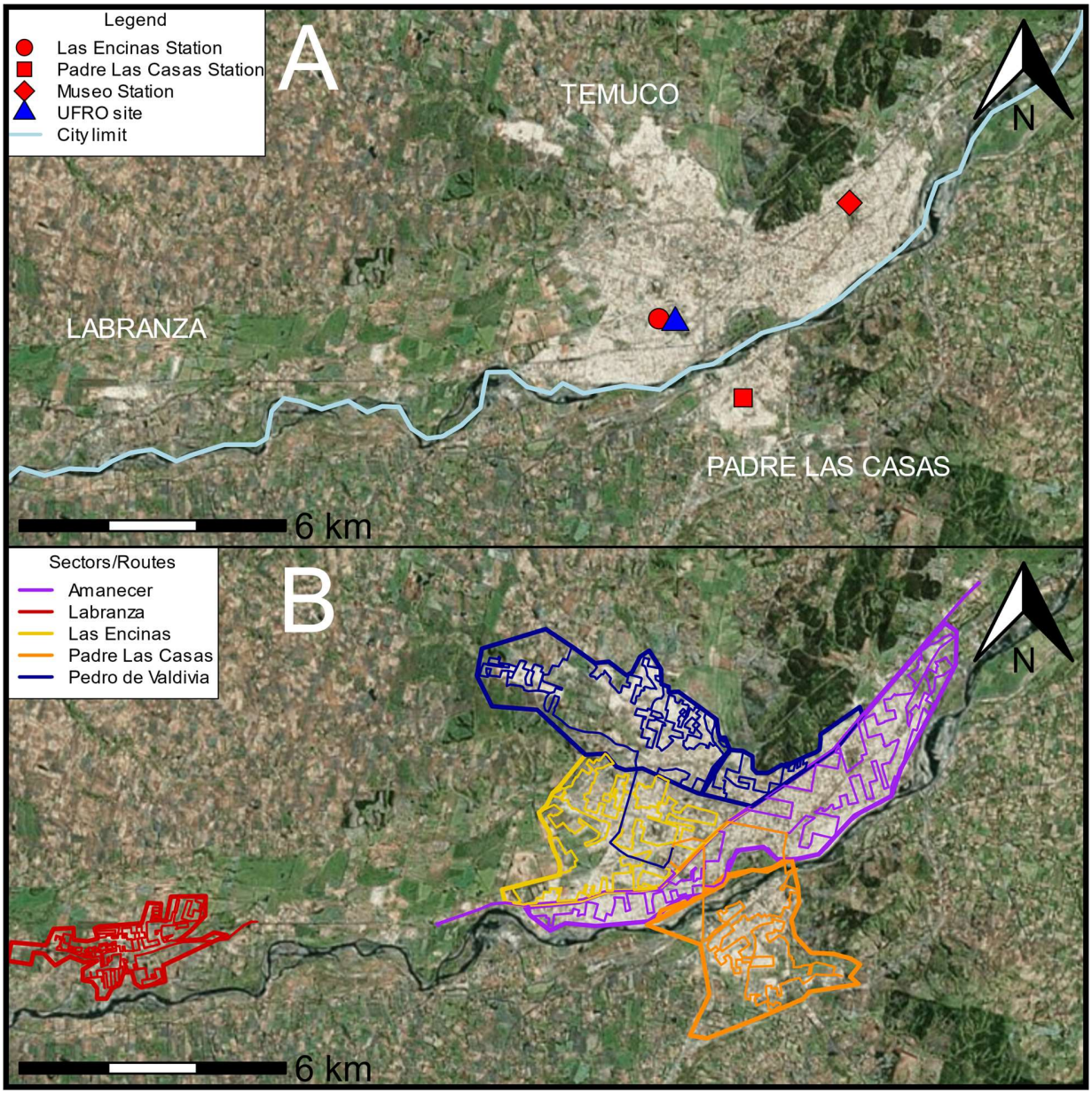

Figure 1. A) Map of study area, including central air quality monitoring site (red circle) and two other monitoriting sites (red square and red diamond), nightly starting point Universidad de la Frontera (blue triangle), and Cautín river that separates Temuco from Padre Las Casas (light blue line that represents the border between municipalities). B) Monitoring routes, delineated with different colors.

The Temuco urban area has an oceanic climate with average mild temperatures (~12° C), warm summers (December to March) and cold winters (May to August) and high

annual precipitations throughout the entire year (~1,000 mm) with highest levels in July and August (winter), October (spring), and December (summer) (44). The Araucanía region is one of the poorest in Chile with lower average years of schooling and a higher percentage of incomplete secondary education compared to national averages (45). The main economic activity is agriculture with some processed-wood industries (39,46–48).

The Temuco urban area experiences extreme air pollution episodes, particularly in winter due to poor dispersion conditions, which facilitate the accumulation of air pollutants (39). The largest aggregated source of air pollution is residential wood-burning with other sources, such as traffic emission or industry, being relatively low (46). It is estimated that more than 88 % of homes have woodstoves, using approximately 654,000 m^3 of wood per year (9,46,49,50). Local mitigation plans include the restriction of wood-burning in defined polygons within the city limits.

2.2 Monitoring campaign

2.2.1 Mobile and central site monitoring.

Data for hourly $PM_{2.5}$ and meteorology (temperature, relative humidity, and wind speed) were obtained from the Las Encinas Station run by the government (51). Las Encinas is a centrally located site in a residential area close to some busy streets, but not highways. Mobile $PM_{2.5}$ was measured using handheld optical particle counters (DUST-TRAK II, Model 8532, TSI, Shoreview, MN, USA), while UFP was measured using handheld condensational particle counters (P-TRAK Model 8525, TSI). DUST-TRAK II was operated with the 2.5 µm size selective impactor. Position was recorded using handheld GPS devices (Garmin 60CSx) and a recording device was used to document

197 fires and other important episodes that might influence monitoring. All instruments were
198 housed in a backpack and placed in the front seat of a compact vehicle with an inlet tubing
199 connected to the outside air through the window (Figure S 1), which kept the instrument
200 warm and controlled the effect of relative humidity on concentrations (23,26,32). Sample
201 air was collected through a tube provided by the manufacturer (3 feet, 1/8 inch internal
202 diameter conductive tubing, for Dust-Trak, and 4 feet, 1/8 inch Tygon tubing for P-Trak).
203 Metal covers were placed around the inlet to protect it from rain and a metal screen was
204 placed in front of the inlet to avoid the intake of large debris or insects. All instruments
205 were set to record every one second. To control for temporal variations in background
206 levels, another pair of Dust-Trak and P-Trak instruments were set up at a central site at
207 the Las Encinas Campus of the University of La Frontera approximately one km from the
208 nearest government monitoring site (Figure 1 A), located in a residential area
209 approximately 0.5 km from the nearest busy road. Samplers were placed in a room at the
210 1-story building of the Environmental Institute (*Instituto del Medio Ambiente*) of the
211 Universidad de la Frontera with inlets extending to the exterior of the building from a
212 window three meters high and as far away from surfaces as possible. DustTrack
213 measurements were very similar to those measured at the government monitoring station
214 (central site), see Figure S 2.
215
216 *2.2.2 Monitoring sessions.*
217 Daily monitoring sessions were performed during winter nights from 20:00 to 2:00 (6-hour
218 periods), similar to most mobile studies of wood-burning, as at this time traffic emissions
219 are generally lower (work day ends and traffic peaks at 18:00) (52) and wood-burning
220 emissions are greatly increased (33,39,53). Before and after each session, quality control

procedures were performed at the central site, which included zeroing the monitors using a filter, as recommended by the manufacturer, and collecting three minutes of collocated data at the central site (of both the mobile and the central site monitors), in order to correct readings between instruments. During a typical session, the vehicle followed prescribed routes for 2 hours, followed by a 30-minute break and 2 additional hours of monitoring. Each session ended with data download and back up on a computer and a separate storage device.

2.2.3 Designated routes.

The route was traveled by car at an average speed of 40 km / hr. Two people were in the car at all times: the driver and an assistant in charge of registering unusual traffic, proximity to other sources of emissions, and instrument checking. Data was saved every 30 minutes. Teams monitored equipment every 15 minutes to check whether they were on or were showing error messages. Five routes were drawn to cover most of the urban area under study (Figure 1 B). The urban area was first divided in four polygons. Routes were drawn inside polygons to maximize the variation of potential predictors (wood stove density, population, and elevation) mapped from the 2002 census and mixing the use of main and local streets inside residential neighborhoods (see Figure S 3). An additional route covering Labranza was added, which crossed the town (north to south and east to west) and included out-of-town rural areas to gauge background air pollution levels. Routes were named based on the city or town (e.g., “Padre Las Casas” and “Labranza”) or main neighborhood they represented (e.g., “Amanecer”, “Las Encinas”, “Pedro de Valdivia”, see Figure 1 B).

2.3 Data analysis

Daily data collected was stored as csv files and combined in Excel sheets. To make portable $PM_{2.5}$ measurements comparable with governmental air pollution measurements, a daily correction factor was applied which was calculated using the daily 6-hour measurements of both central site Dust-Trak and the Las Encinas government station. Then, to make portable monitors comparable, a second correction factor was applied to the mobile instruments using the initial and final collocation data; for UFP monitors, only the latter correction was applied (details of procedures are provided in supplemental material and daily correction factors are provided in Table S 1). To better identify zones of higher concentrations considering temporal variations, the ratio between mobile and the central site measurements was calculated for each observation of the trip. The final master file included air pollutants (both as concentrations and ratios), GPS positioning, and information on date, time, and route. All individual trips were initially plotted both as time-series and maps, and visually inspected to spot obvious artifacts such as concentrations that were stuck over time, steady zeros or negative concentrations.

To better estimate spatial distribution of pollutants and to summarize spatial and temporal information, a spatial analysis was conducted by collapsing spatial data in grids (rasters) of different cell sizes (19,36). Four rasters over the whole study area were created with cell sizes of 50, 100, 200, and 400 meters. Then, all individual trips were aggregated within the rasters sequentially by hour, day, and overall period as explained below. Hourly, daily and overall period rasters were plotted over area maps and cells were colored using quantiles.

i) Hourly collapse: all measurements recorded for a certain hour and day were collapsed inside each cell of the raster. The statistics used were the mean and number of observations. Hourly data included the full clock hour (i.e., the collapse for 20:00 hours represents average measurements in each cell for all measurements between 20:00:00 and 20:59:59 hours). An example of the collapse in 200m cells is shown in Figure S 4a for $PM_{2.5}$. It can be seen that both $PM_{2.5}$ concentrations and ratios were nearly normally distributed, while number of observations per cell were log-normally distributed, usually with many observations (>20) per cell.

ii) Daily collapse: for each cell, data from all hourly rasters within a day were collapsed, by the mean. Thus, the daily mean represented the average in each cell for hours 20:00, 21:00, 22:00, 23:00, 0:00, 1:00 and 2:00 obtained from step i). An example is provided in Figure S 4b. Concentrations and number of observations tended to be log-normally distributed, with mean count per cell usually well above 20.

iii) Overall collapse: for each cell, data from all daily rasters obtained in step ii) were collapsed, by the mean concentrations and number of observations. Thus, the overall mean represented the average in each cell of all days that had measurements (with a maximum of 20 days), while counts represented the number of days with observations for the whole period in each cell. An example for $PM_{2.5}$ in 200m cell rasters is provided in Figure S 4c. Concentrations and ratios tended to be log-normally distributed. Also, the distribution of days with observations per cell can be seen, with higher counts in zones of the city more frequently passed and with other parts with 1-2 observation days.

291 To assess the impact of meteorological conditions and number of observations, we
292 also included, as sensitivity analyses, plots excluding rainy days, excluding foggy days
293 and excluding cells with less than 3 observations per cell when collapsing each hour and
294 cells with less than 3 days of observations when collapsing all days (Figure S 5a and 5b).
295 As raster distribution seemed log-normal, daily and overall rasters were characterized by
296 median and quartiles from all individual cell values. Daily raster distributions were grouped
297 by temporal variables (routes, wind speed, temperature and relative humidity, monitoring
298 route) and summary statistics were calculated. To asses statistical differences between
299 groups ANOVA tests were performed, which compared median daily raster values.
300 Global Moran's I statistic was used to estimate the spatial autocorrelation of pollutants
301 with the spatial weights created by the first order queen contiguity rule (54). Moran's I
302 ranges from -1 to 1, where values closer to 1 represent high positive autocorrelation
303 (clustering of similar values), values closer to -1 represent high negative autocorrelation
304 (dispersion), and values close to 0 indicate a random spatial distribution. We performed a
305 Global Moran test to assess whether the observed I was significantly different than 0. We
306 also used the Local Moran's I as a local indicator of spatial association, particularly to
307 detect hotspots (high pollution cells surrounded by other high pollution cells) and coldspots
308 (low pollution cells surrounded by other low pollution cells). Kendall W-statistic was used
309 to determine the agreement (1: perfect agreement, 0: no agreement) between clusters
310 found for $PM_{2.5}$ and UFP (55).
311 To identify zones of the city where hotspots were more frequent, data was also
312 collapsed by neighborhood using a polygon of 44 neighborhood units (*unidades*
313 *vecinales*). These are administrative units inside municipalities that tend to represent
314 homogeneous neighborhoods. Hotspots cells were collapsed by neighborhood, by

estimating the percent of the area of the unit with actual measurements comprised by hotspots cells. Neighborhoods with more than 20% area comprised by hotspot cells were considered as having high presence of hotspots. Additionally, socioeconomic status (SES) was obtained inside each unit by estimating the percent of block areas where homes with certain purchasing power (0 to 4) are dominant with 0 being the highest SES and 4 the lowest SES (56). To evaluate the potential association between presence of hotspots and SES, we fitted a regression model of percent area of hotspots against percent area of high or low SES. For comparison purposes, the polygons of wood-burning restrictions were added to the maps. All analyses were conducted using R software (57) using the "raster" package for raster analyses and the "spdep" package was used for cluster detection .

3. Results and Discussion

3.1 Air pollution and meteorology in Temuco

A total of 20 sessions were performed on weekday nights between May 26th and July 15th 2016 covering all five routes a similar number of times (Table S 2). Summary statistics of $PM_{2.5}$, temperature, relative humidity, and wind speed measured at the central site over the course of the 20 mobile monitoring sessions are shown in Table 1. During the monitoring nights, temperatures were on average 8º C, with relative humidity of 94 % and wind speed < 1 m/s, conditions that favor the use of heaters and accumulation of pollutants. Overall, levels of $PM_{2.5}$ were very high (135.4 μg m^{-3}, on average) with wide variation indicated by a large standard deviation (125.4 μg m^{-3}). These $PM_{2.5}$ levels were nearly double the reported levels for the capital city of Santiago (20), which is reflective of wood burning for heating that occurs in Temuco and not in Santiago (11,12). Air quality

standards in Chile are more lenient than those standards of the Environmental Protection Agency (EPA) and the World Health Organization (WHO) with daily concentrations of $PM_{2.5}$ not to exceed 50 µg m^{-3}, compared to 35 and 15 µg m^{-3}, respectively (58–60). Similar summary statistics were observed when grouping by route (Table S 3). In addition, Figure S 6 shows boxplots of $PM_{2.5}$, wind speed, temperature, and relative humidity by hour measured at the central site. Median $PM_{2.5}$ was highest at 20:00 and 21:00 hours and decreased after 21:00, along with temperature, which is consistent with our previous work (39) and has been observed in most of similar studies (33,53). Wind speed remained low during sampling period. $PM_{2.5}$ levels reflect the regional context of residential wood-burning in the colder seasons (6,7) in the south of Chile, where wood is significantly cheaper than natural gas, for example (14,15).

Table 1. Central Site Summary Statistics

Variable	N*	Mean	SD	Min	Max	p5	p95
$PM_{2.5}$ (µg/m^3)	120	135.4	125.4	9.5	573.3	19.7	441.8
Temperature (°C)	120	7.7	1.8	3.5	11.7	4.5	10.4
Relative Humidity (%)	103	94.1	6.4	78.1	100.0	80.1	100.0
Wind Speed (m/s)	118	0.9	0.7	0.0	3.2	0.1	2.3

*Hourly observations; SD: standard deviation; p: percentile

3.2 Spatial and temporal distribution of air pollution

Mobile measurements were collapsed within the raster cells. Table 2 shows summary statistics for mobile $PM_{2.5}$ and UFP concentrations, and ratios compared to the central site in 200m-cells rasters (Table S 4a- S 4d show statistics per day). Mobile measurements of $PM_{2.5}$ concentrations were high with large variability (median 97.6, 1st and 3rd quartile 47.7 and 109.9, µg m^{-3}), with ratios slightly below one (median 0.8, 1st and 3rd quartile 0.6 and

358 1.0), which indicates that the concentration were slightly lower on average, to central site
359 measurements. Previous studies either in rural/suburban (25,26,31,33,34) or urban
360 (23,35,36,61) found $PM_{2.5}$ concentrations much lower than this study, with mean
361 concentrations in areas ~10-20 μg m^{-3} and ~20 μg m^{-3} in most impacted areas. Only Allen
362 (2011) reported peaks >100 μg m^{-3} in heavily impacted areas (26). For UFP,
363 concentrations measured via mobile sampling were lower (median ~30.000 counts cm^{-3})
364 than those reported for the Metropolitan Region of Santiago (20), which is understandable
365 as Santiago is a larger city with nearly 7 million inhabitants and a much larger vehicle fleet
366 (62). Levels were somewhat lower than that reported to be measured in street canyons
367 and higher than those reported in other urban areas (63,64). The relatively large
368 concentrations might be due to an older fleet of diesel buses and trucks, as it is known
369 that both the proportion of diesel cars and the sulfur content of diesel in Chile is low (65).
370 Mean ratio of UFP compared to the central site were higher than 1, indicating that mobile
371 measurements were, in general, higher than the central site. When comparing routes, we
372 observed variations in the concentrations and ratios for $PM_{2.5}$ across the five routes (ratio
373 of 1.2 for Las Encinas compared to 0.6 for Labranza), but differences were not statistically
374 significant. Some differences were also found for UFP, but in the opposite direction of that
375 observed for $PM_{2.5}$ (e.g., Labranza presented the highest UFP ratio with 1.3). Regarding
376 meteorological variables, concentrations tended to be higher with higher relative humidity,
377 lower temperatures and lower wind speed but did not reached statistical significance
378 (except for temperature and $PM_{2.5}$), while ratios were less influenced by meteorological
379 conditions. Overall, these trends can be explained by noting that these conditions favor
380 residential wood-burning and pollutant accumulation throughout the urban area.

Table 2. Summary statistics of overall mobile pollutant measurements by route and meteorological variables. Each observation summarizes a daily 200m cell raster

	Mobile Pollutant Measurements											
	$PM_{2.5}$ (μg m^{-3})			$PM_{2.5}$ ratio[1]			UFP (# cm^{-3})			UFP ratio[1]		
Category	**N**	**Median (Q1-Q3)**	**pv[2]**	**N**	**Median (Q1-Q3)**	**pv[2]**	**N**	**Median (Q1-Q3)**	**pv[2]**	**N**	**Median (Q1-Q3)**	**pv[2]**
Overall	20	97.6 (47.7-109.9)	NA	20	0.8 (0.6-1.0)	NA	19	31,432 (19,505-44,145)	NA	19	1.2 (1.0-1.4)	NA
Route												
Amanecer	4	73.8 (67.2-83.8)	0.61	4	0.9 (0.7-1.2)	0.68	3	22,857 (19,416-25,119)	0.79	3	1.2 (0.9-1.5)	0.85
Labranza	4	93.3 (81.2-104.2)		4	0.6 (0.6-0.6)		4	45,312 (41,644-54,263)		4	1.3 (1.2-1.4)	
Las Encinas	4	135.2 (45.2-191.2)		4	1.2 (0.9-1.5)		4	28,419 (16,683-41,489)		4	1.3 (1.1-1.5)	
Padre las Casas	4	84.4 (38.2-111)		4	0.7 (0.6-0.8)		4	28,559 (19,093-36,487)		4	1.0 (0.9-1.2)	
Pedro de Valdivia	4	101.4 (46.7-136.5)		4	0.8 (0.6-1.0)		4	29,870 (18,072-38,238)		4	1.1 (0.9-1.3)	
Relative Humidity												
<95%	8	79.6 (38.2-109.9)	0.35	6	0.7 (0.6-0.9)	0.64	6	22,586 (18,419-19,970)	0.43	6	1.1 (1.0-1.2)	0.84
>95%	10	115.4 (57.5-154.1)		12	0.9 (0.7-1.2)		11	34,694 (25,119-44,145)		11	1.2 (1.0-1.4)	
NA	2	80.8 (80.5-81.2)		2	0.6 (0.6-0.7)		2	40,030 (32,171-47,889)		2	1.4 (1.2-1.5)	
Temperature												
<7.5 °C	10	133.5 (80.5-166.2)	**0.04**	10	0.8 (0.6-1.0)	0.72	10	38,047 (30,471-45,456)	0.22	10	1.2 (1-1.3)	0.69
>7.5 °C	10	61.8 (37.4-96.1)		10	0.9 (0.6-1.1)		9	24,083 (18,335-20,497)		9	1.3 (1-1.4)	
Wind Speed												
<1 m/s	13	119.8 (77.5-151.2)	0.11	12	0.8 (0.6-1.0)	0.99	11	40,187 (31,202-50,595)	0.13	11	1.2 (1.0-1.4)	0.85
>1 m/s	7	56.6 (36.6-71)		8	0.9 (0.7-1.0)		8	19,395 (16,661-21,240)		8	1.2 (1.0-1.3)	
Wind Direction												
E	13	95.4 (51.1-108.9)	0.71	13	0.9 (0.7-1.0)	0.79	12	30,141 (19,641-40,178)	0.79	12	1.1 (1.1-1.3)	0.87
N	1	102.7 (102.7-102.7)		1	0.6 (0.6-0.6)		1	53,769 (53,769-53,769)		1	1.3 (1.3-1.3)	
S	3	63.3 (38.5-75.8)		3	0.8 (0.6-0.9)		3	23,944 (19,584-26,580)		3	1.2 (0.9-1.4)	
W	3	140.1 (54.5-196.4)		3	0.9 (0.6-1.1)		3	36,639 (27,084-51,258)		3	1.4 (1.2-1.6)	

[1] Ratio compared to central site; [2] ANOVA comparisons between groups. Q1: first quartile (25% percentile). Q3: third quartile (75% percentile).

To determine areas of the city with higher local concentrations, only ratios were analyzed. Table 3 provides summary statistics for $PM_{2.5}$ and UFP ratios for the overall rasters by cell size. $PM_{2.5}$ ratios were around 1 with a decreasing trend for larger cell sizes. UFP ratio, on the other hand, were systematically above 1 (around 1.3), regardless of the cell size. This may be due to the local impacts of UFP sources, such as mobile emissions, affecting more the mobile measurements than the central site. Very large spatial variation was observed for ratios of both $PM_{2.5}$ and UFP, given the large standard deviations and differences in percentiles (5^{th} and 95^{th}), with differences up to 4-fold when comparing more polluted to less polluted areas.

Table 3. Summary statistics of pollutant ratio to central site by spatial resolution

	Statistics within cells			
Resolution	**N cells**	**Median**	**5th percentile**	**95th percentile**
$PM_{2.5}$ ratio[1]				
50 m	7611	0.89	0.23	2.30
100 m	3059	0.89	0.26	2.13
200 m	1077	0.85	0.27	1.93
400 m	355	0.82	0.26	1.75
UFP ratio[1]				
50 m	7856	1.24	0.44	2.53
100 m	3137	1.25	0.46	2.46
200 m	1092	1.27	0.48	2.29
400 m	355	1.29	0.52	2.09

[1] ratio of measurement compared to central site

Figure 2 shows ratios of $PM_{2.5}$ (upper panel) and UFP (lower panel) at a 200-meter spatial resolution, including the boundaries of the neighborhoods, that confirmed the heterogenous distribution of $PM_{2.5}$ and UFP ratios, suggesting clustering within the urban area. Specifically, some sectors recorded levels of $PM_{2.5}$ and UFP nearly half that of the

central site (darkest blue tone), while other neighborhoods had nearly twice the level recorded at the central site (darkest red tone). An initial observation is that for both $PM_{2.5}$ and UFP, concentrations drop to very low values when leaving urban areas, likely reaching regional background levels of a few μg m^{-3} of $PM_{2.5}$ and few thousand counts cm^{-3} of UFP (Figure S 7). This pattern of dropping to very low levels when leaving the urban areas affected by wood-burning emission was also observed by other authors (25,26). Higher ratios for $PM_{2.5}$ were mainly clustered in the western part of the city and also in the east and the satellite city of Labranza, while for UFP, ratios seem to cluster slightly similar to $PM_{2.5}$, but with higher ratios across the city and grouped near major highways, particularly toward Labranza (section of map between starting at the neighborhood Amanecer and continuing to Labranza).

Most of the higher ratio areas fell within the wood-burning restriction zones, although some large sections were not like those in the south-western part of Temuco. Despite the fact that the government monitoring station in Padre Las Casas was measuring higher concentrations than the Las Encinas station-central site (Figure S 6), we failed to detect higher ratios in the Padre Las Casas route although the area is known to present higher concentrations than areas of Temuco (66). Time-series data was reviewed and no unusual observations were observed; however, sampling days were mostly foggy and rainy, which could have led to artifactual measurements in some of the instruments. It is also possible that the Padre Las Casas station is located in an area locally impacted by PM, as could be inferred by Figure 2 and Figure S 6.

Figure S 5a shows plots for $PM_{2.5}$ in 200-m rasters for a variety of conditions like including days with no rain, days without fog and cells that meet certain minimal numbers

of observations (see methods). In general, the pattern seems similar to the original analysis, with all data, which is also evidenced by regressions plots shown on Figure S 5b. Portions of the city, toward the south (with some part of Padre Las Casas) and the north, are lost due to scarcity of data, which might mean that reported observations in these zones might be unstable.

A trend towards the clustering of UFP concentrations around major highways is more clearly evident when plotting 100m rasters (Figure S 8). Also, lower $PM_{2.5}$ levels, but not UFP, were observed in downtown neighborhoods (Caupolicán, Centro, Las Heras, Balmaceda) which can be explained by the higher frequency of commercial zones and high-rise residential buildings, implying lower frequency of residential woodstoves. A similar pattern was observed by Larson at colleagues in Vancouver (23).

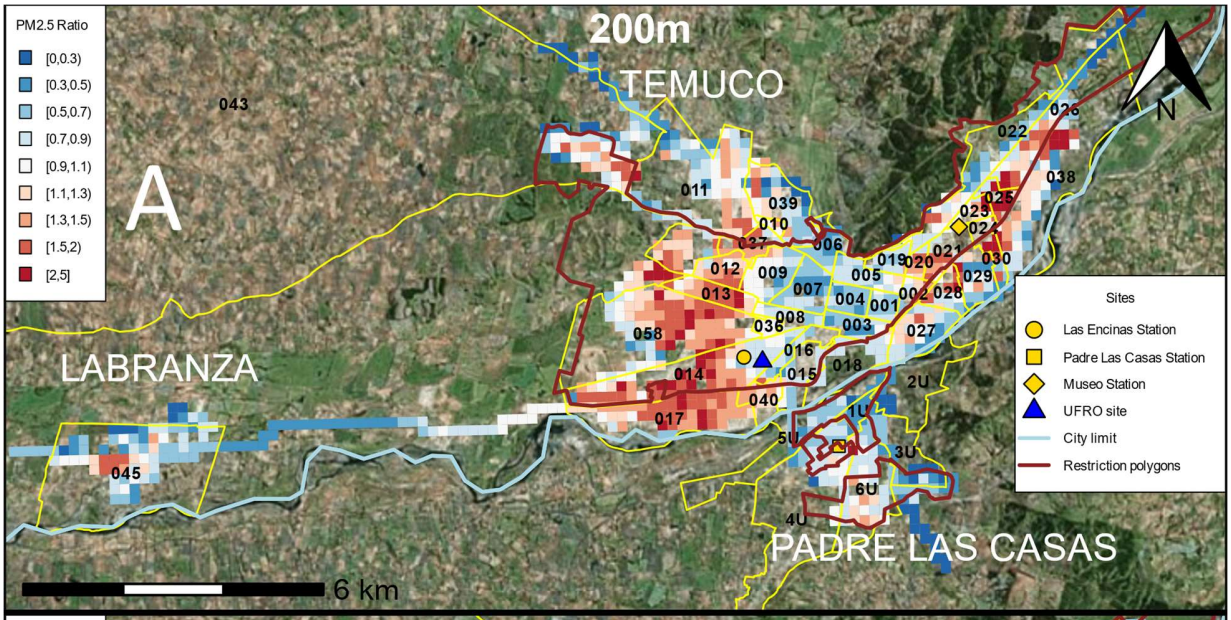

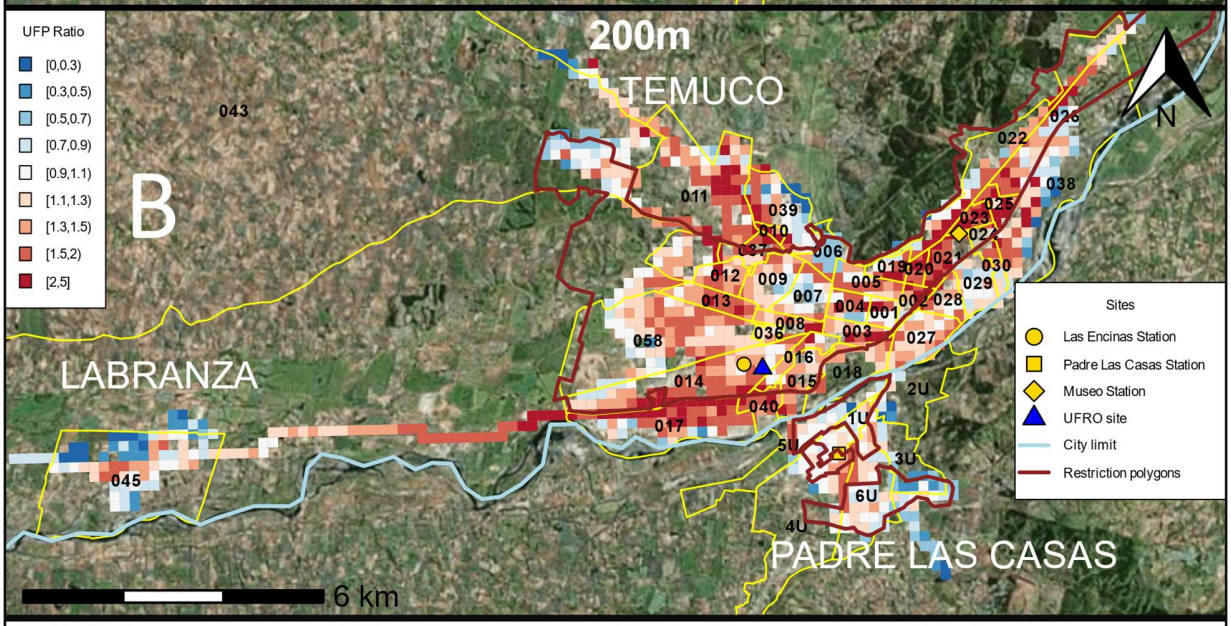

Neighborhood

009-HUICHAHUE
1U-VILLA ALEGRE
2U-LA UNION
3U-ALIANZA
4U-THIERS
5U-RIBERENOS
6U-MAQUEHUE
001-CENTRAL
002-ESTACION
003-LAS HERAS
004-CAUPOLICAN
005-BALMACEDA
006-PEDRO DE VALDIVIA
007-LOS JARDINES
008-DREVES
009-SOFO
010-LOS LAURELES
011-TROMEN
012-IGUALDAD Y TRABAJO
013-MILLARAY
014-UNIVERSIDAD
015-LAS QUILAS
016-IMPERIAL
017-AMANECER
018-PICHI CAUTIN
019-LOURDES
020-TUCAPEL
021-MAESTRANZA
022-5 DE ABRIL
023-ERNESTO BOHN
024-NIELOL
025-EVARISTO MARIN
026-PORVENIR
027-SAN ANTONIO
028-PAREDES
029-SANTA ROSA
030-POMONA
036-ESTADIO
037-CAMPOS DEPORTIVOS
038-VILLA TURINGIA
039-VISTA HERMOSA
040-VILLA SUR
058-JOSE MIGUEL CARRERA
043-TROMEN MOLULCO
045-LABRANZA

Figure 2. Ratios of $PM_{2.5}$ (A) and UFP (B) (mobile-measured concentrations compared to central site) at a 200-meter spatial resolution with neighborhoods indicated by number. Ratios above 1 are colored in orange-red tones (darker red color indicates a higher ratio) and ratios below 1 are colored in blue tones (darker blue tone indicates lower ratio).

3.3 Spatial analysis

We calculated the spatial autocorrelation at cell sizes of 50, 100, 200 and 400 m, and found strong positive and statistically significant autocorrelation at each size (Table 4) for ratios of $PM_{2.5}$ and UFP to the central site of similar magnitudes (between 0.6 and 0.7). Autocorrelations tended to decrease as the cell size increased, but remained high for all cell sizes, indicating that clustering was slightly higher at smaller sizes for both contaminants. This general observation supports the notion that concentrations can be clustered.

Table 4. Global Moran's I Results

Pollutant	**Resolution**	**Moran's I**	**p-value[1]**
$PM_{2.5}$ ratio	50 m	0.717	**<0.001**
	100 m	0.653	**<0.001**
	200 m	0.657	**<0.001**
	400 m	0.644	**<0.001**
UFP ratio	50 m	0.617	**<0.001**
	100 m	0.508	**<0.001**
	200 m	0.534	**<0.001**
	400 m	0.493	**<0.001**

[1] Global Moran Test

Hotspots and coldspots were identified through the local Moran's I. Figure 3 shows distributions of local Moran's I for ratios of $PM_{2.5}$ (panel A) and UFP (panel B) at a 200-m cell size, with hotspots colored in red and coldspots in blue. We confirmed the presence of $PM_{2.5}$ hotspots in central/west neighborhoods, and some in the eastern area of the city (e.g., Evaristo Marin neighborhood). With respect to UFP, clusters of higher ratios tended to appear in the outer portions of the urban area (Amanecer), which may be indicative of higher road traffic and also some neighborhoods in the eastern region of the city.

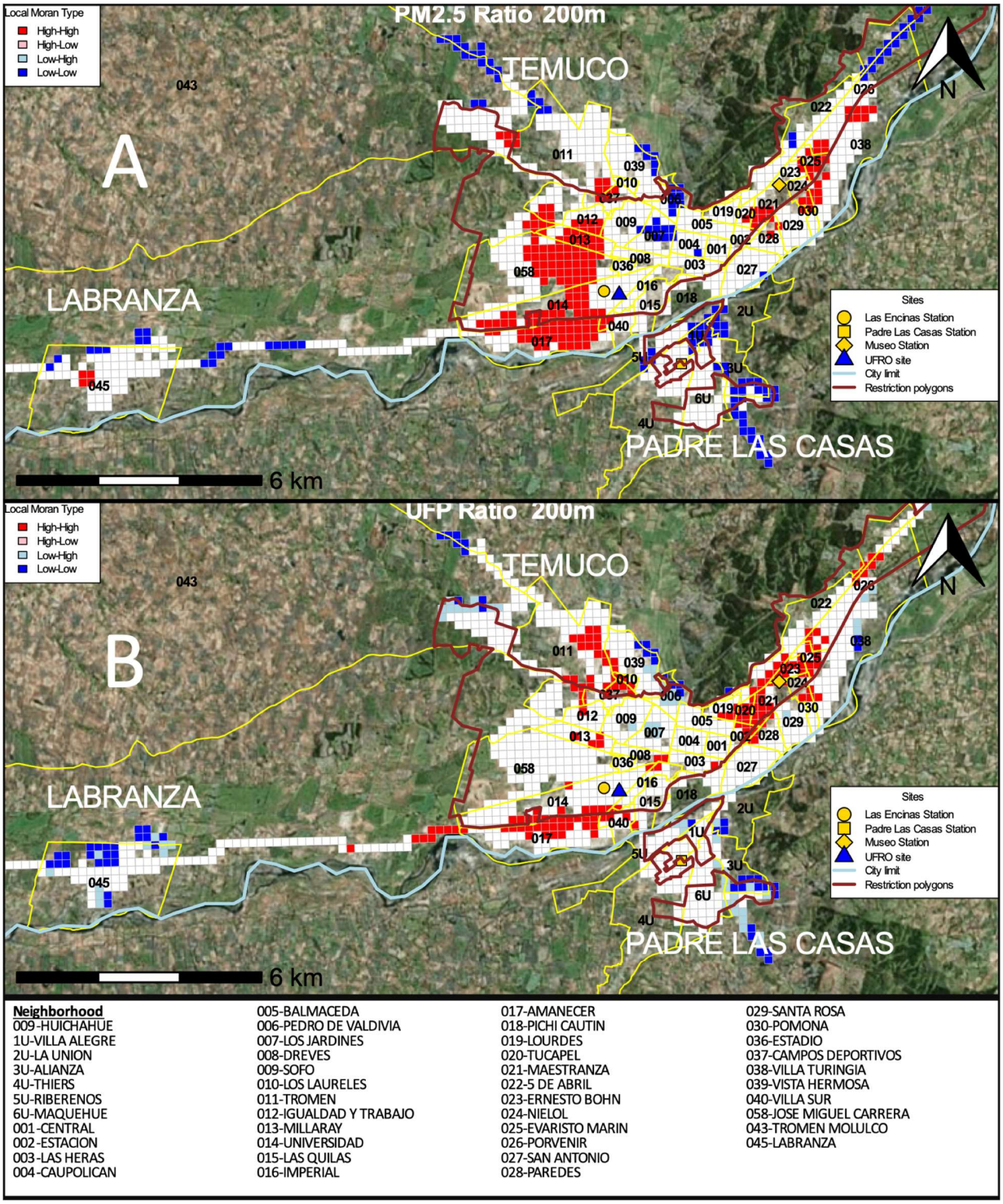

Figure 3. Clusters of $PM_{2.5}$ (A-upper panel) and UFP (B-lower panel) ratios to central site at 200m cell size. Hotspots are colored in red and cold spots in blue.

Table S 5 provides information on the percent area being hotspots in each neighborhood for ratios of $PM_{2.5}$ and UFP at a 200-m spatial resolution. From a total of 43 neighborhoods in Temuco, 14 neighborhoods were classified as having high presence of hotspots for $PM_{2.5}$, and 19 neighborhoods for UFP (bolded in Table S 5). Hotspots were particularly concentrated in the Evaristo Marin, Maestranza, and Maquehue neighborhoods, where 75% of the neighborhood area was categorized as a hotspot for $PM_{2.5}$. For UFP, the Ernest Bohn, Maestranza, and Universidad neighborhoods were particularly affected (>85% of the area classified as a hotspot for UFP). We failed to detect an association between the presence of hotspots and SES (Figure S 9).

Eleven neighborhoods simultaneously contained hotspots for both pollutants (shaded in grey in Table S 5). We tested the spatial agreement between clusters (hotspots and cold spots) of $PM_{2.5}$ and UFP using the Kendall W. We observed significant agreement ($p<0.001$), but with an intermediate Kendall W value of 0.602 and weak Spearman correlation coefficient of 0.203. This partial agreement is expected as wood burning emits at rather large particle sizes (41,42) and the places of agreement could be where traffic emission (contributing both $PM_{2.5}$ and UFP) are clustered. One previous study documented the lack of agreement of $PM_{2.5}$ and UFP in a setting impacted by wood-smoke (34).

4. General Discussion

Understanding spatial variation is important. At a general level, spatial variation can identify local hotspots of air pollution often masked by reliance on stationary air quality monitors. Thus, detecting hotspots may help focus reduction efforts. In the current case

of the Temuco urban area, these results may assist in targeting specific air pollution mitigation strategies. Like many southern Chilean cities, Temuco has been declared a “saturated area” for PM and has an Air Pollution Management Plan in place to direct public policy efforts to significantly reduce air pollution (46). Major policy efforts include improving thermal insulation of homes and replacing less efficient wood-burning stoves (67). Despite significant efforts by local and national authorities, PM levels have not be significantly reduced in the last 5 years (39). In the work conducted in another southern Chilean city, Valdivia, Reyes et al. suggest that social inequalities and energy consumption patterns should be considered in the implementation of air quality mitigation policies (37). In addition, studies are needed to test whether insulation improvements and stove replacement policies might be more effective if they were spatially-implemented (e.g., based on hotspots of air pollution). Our work may be used to guide reduction efforts.

Some limitations of our work should be considered. First, results were obtained with a rather limited number of days, with about four repetitions in each neighborhood. Van den Bossche suggested that more consistent spatial results (errors of approximately 50 %) could be obtained by including 5-11 repetitions (22). Our results are at the lower end of the suggestion, but included a correction for a central site measurement, which likely increased precision. Additionally, the differences in ratios observed were of about 2 to 3 times between areas of higher and lower ratios, which are much higher than the 50% proposed error. Finally, the results allowed for the identification of likely clusters of pollutants, which could be further studied with more extensive spatial sampling. Second, many sampling nights presented high relative humidity and instruments did not have inlets to reduce humidity. As a result, it is possible that measurements were altered (Table S

1), however, much of the effect should be reduced by keeping instruments warm inside the vehicle, as others have argued (23,32,33,52) and also it is unlikely it could explain the large observed variations. In any case, information for some sections of the city may be unstable as they were affected by meteorological conditions and a limited number of observations. It might be advisable to run sampling campaigns for different meteorological conditions and assess the stability of clusters. Finally, although the current work might be valid for the observed period, it remains to be studied how much a short sampling campaign, like the one presented here, might represent clusters in a longer time frame and under different meteorological condition.

5. Conclusions

We present the results of a winter mobile campaign in Temuco, Chile, a city heavily impacted by residential wood-burning. Very large and intermediate concentration levels were observed for $PM_{2.5}$ and UFP, respectively. Temporal effects were controlled by expressing spatial levels as ratios to central site. By collapsing results in spatial grids, we showed that pollutants were distributed unevenly around the city, with $PM_{2.5}$ clustered around more residential areas and UFP in zones more impacted by traffic. Through spatial statistical methods, clusters (hotspots) of pollutants were identified for the time period within grids along with neighborhood with high percent area of hotspots. From 44 neighborhoods, about 10 to 20 had hotpots for either pollutant with weak agreement between pollutants. Indicators of neighborhood SES were not associated with hotspots in our initial analysis, however, a more nuanced evaluation of how SES may relate to the

distribution of air pollution is warranted. The very large concentrations of $PM_{2.5}$ indicate the need to implement extensive reduction plans in order to protect the health of the population. The current work presents a cost-effective way to initially characterize the spatial distribution of pollutants and likely clusters for a time period, which may guide future spatial campaigns and help target local interventions aimed at air pollution mitigation.

Acknowledgements

This work was supported by “Impact of Wood-burning Air Pollution on Preeclampsia and other Pregnancy Outcomes in Temuco, Chile” (DPI2140093) by CONICYT and Research Councils UK. Estela Blanco, María Elisa Quinteros, and Salvador Ayala were supported by a doctoral scholarship by ANID Beca Doctorado Nacional No. 21201332, No. 21150801 and No. 21191111, respectively. Juana Maria Delgado-Saborit was supported by the European Union’s Horizon 2020 research and innovation programme under the Marie Skodowska-Curie grant agreement No. 750531.

Competing financial interests

The authors declare they have no competing interests.

References

1. Álvarez B, Boso Á. Representaciones sociales de la contaminación del aire y las estufas de leña en diferentes niveles socioeconómicos de la ciudad de Temuco, Chile. Rev Int Contam Ambient. 2018;34(3):527–40.
2. Goldemberg J, United Nations Development Programme. United Nations. Department of Economic and Social Affairs, World Energy Council. World energy assessment: energy and the challenge of sustainability. United Nations Development Programme; 2000. 508 p.
3. WHO, Regional office for Europe. Residential heating with wood and coal: health impacts and policy options in Europe and North America. 2015. Available from: https://www.euro.who.int/en/publications/abstracts/residential-heating-with-wood-and-coal-health-impacts-and-policy-options-in-europe-and-north-america
4. Brauer M, Allen G. Modeling Pollution from. Air Waste Manag Assoc. 2010;(May):24–8.
5. Naeher LP, Brauer M, Lipsett M, Zelikoff JT, Simpson CD, Koenig JQ, et al. Woodsmoke health effects: A review. Inhalation Toxicology. 2007; Jan;19(1):67-106.
6. Díaz-Robles LA, Fu JS, Vergara-Fernández A, Etcharren P, Schiappacasse LN, Reed GD, et al. Health risks caused by short term exposure to ultrafine particles generated by residential wood combustion: A case study of Temuco, Chile. Environ Int. 2014;66:174–81.
7. Jorquera H, Barraza F, Heyer J, Valdivia G, Schiappacasse LN, Montoya LD. Indoor PM2.5in an urban zone with heavy wood smoke pollution: The case of Temuco, Chile. Environ Pollut. 2018;236:477–87.
8. Prieto-Parra L, Yohannessen K, Brea C, Vidal D, Ubilla CA, Ruiz-Rudolph P. Air pollution, PM2.5 composition, source factors, and respiratory symptoms in asthmatic and nonasthmatic children in Santiago, Chile. Environ Int. 2017 Apr;101:190–200.
9. Villalobos AM, Barraza F, Jorquera H, Schauer JJ. Wood burning pollution in southern Chile: PM 2.5 source apportionment using CMB and molecular markers. Environ Pollut. 2017;225:514–23.
10. Cakmak S, Dales RE, Vida CB. Components of particulate air pollution and mortality in Chile. Int J Occup Environ Health. 2009;15(2):152-8
11. Díaz-Robles L, Díaz-Robles L, Cortés S, Carlos Ortega J, Vergara-Fernández A. Short term health effects of particulate matter: A comparison between wood smoke and multi-source polluted urban areas in Chile. Aerosol Air Qual Res. 2015;15(1).
12. Sanhueza P a, Torreblanca M a, Diaz-Robles L a, Schiappacasse LN, Silva MP, Astete TD. Particulate air pollution and health effects for cardiovascular and respiratory causes in Temuco, Chile: a wood-smoke-polluted urban area. J Air Waste Manag Assoc. 2009;59:1481–8.
13. SICAM I. Actualización del Inventario de Emisiones Atmosféricas para las comuncas de Temuco y Padre Las Casas, Año Base 2017. Temuco, Chile; 2018.

14. Cortés A, Ridley I. Efectos de la combustión a leña en la calidad del aire intradomiciliario. La ciudad de Temuco como caso de estudio. Rev INVI. 2014;28(78).
15. Schueftan A, González AD. Reduction of firewood consumption by households in south-central Chile associated with energy efficiency programs. Energy Policy. 2013;63:823-32.
16. Van den Bossche J, Theunis J, Elen B, Peters J, Botteldooren D, De Baets B. Opportunistic mobile air pollution monitoring: A case study with city wardens in Antwerp. Atmos Environ. 2016;141:408-21.
17. Su JG, Buzzelli M, Brauer M, Gould T, Larson T V. Modeling spatial variability of airborne levoglucosan in Seattle, Washington. Atmos Environ. 2008;42(22): 5519-25.
18. Gozzi F, Della Ventura G, Marcelli A. Mobile monitoring of particulate matter: State of art and perspectives. Atmospheric Pollution Research. 2016.
19. Li HZ, Gu P, Ye Q, Zimmerman N, Robinson ES, Subramanian R, et al. Spatially dense air pollutant sampling: Implications of spatial variability on the representativeness of stationary air pollutant monitors. Atmos Environ X. 2019;2: 1000012.
20. Suarez L, Mesias S, Iglesias V, Silva C, Caceres DD, Ruiz-Rudolph P, et al. Personal exposure to particulate matter in commuters using different transport modes (bus, bicycle, car and subway) in an assigned route in downtown Santiago, Chile. Environ Sci Impacts. 2014;16(6):1309–17.
21. Sullivan RC, Pryor SC. Quantifying spatiotemporal variability of fine particles in an urban environment using combined fixed and mobile measurements. Atmos Environ. 2014;Jun 1;89:664–71.
22. Van den Bossche J, Peters J, Verwaeren J, Botteldooren D, Theunis J, De Baets B. Mobile monitoring for mapping spatial variation in urban air quality: Development and validation of a methodology based on an extensive dataset. Atmos Environ. 2015;105: 148-161.
23. Larson T, Su J, Baribeau AM, Buzzelli M, Setton E, Brauer M. A spatial model of urban winter woodsmoke concentrations. Environ Sci Technol. 2007;41(7): 2429-2436.
24. Larson T, Henderson SB, Brauer M. Mobile monitoring of particle light absorption coefficient in an urban area as a basis for land use regression. Environ Sci Technol. 2009;43(13): 4672-4678.
25. Smargiassi A, Brand A, Fournier M, Tessier F, Goudreau S, Rousseau J, et al. A spatiotemporal land-use regression model of winter fine particulate levels in residential neighbourhoods. J Expo Sci Environ Epidemiol. 2012; Jul;22(4):331-8.
26. Allen GA, Miller PJ, Rector LJ, Brauer M, Su JG. Characterization of Valley Winter Woodsmoke Concentrations in Northern NY Using Highly Time-Resolved Measurements. Aerosol Air Qual Res. 2011;11(5).
27. Hudda N, Gould T, Hartin K, Larson T V., Fruin SA. Emissions from an international airport increase particle number concentrations 4-fold at 10 km downwind. Environ Sci Technol. 2014;48(12):6628–35.

28. Fruin S, Westerdahl D, Sax T, Sioutas C, Fine PM. Measurements and predictors of on-road ultrafine particle concentrations and associated pollutants in Los Angeles. Atmos Environ. 2008;42(2):207–19.
29. Yu CH, Fan Z, Lioy PJ, Baptista A, Greenberg M, Laumbach RJ. A novel mobile monitoring approach to characterize spatial and temporal variation in traffic-related air pollutants in an urban community. Atmos Environ. 2016;141: 161-173.
30. Loeppky JA, Cagle AS, Sherriff M, Lindsay A, Willis P. A local initiative for mobile monitoring to measure residential wood smoke concentration and distribution. Air Qual Atmos Heal. 2013;6(3):641–53.
31. Thatcher TL, Kirchstetter TW, Tan SH, Malejan CJ, Ward CE. Near-Field Variability of Residential Woodsmoke Concentrations. Atmos Clim Sci. 2014;4(4).
32. Grivas G, Stavroulas I, Liakakou E, Kaskaoutis DG, Bougiatioti A, Paraskevopoulou D, et al. Measuring the spatial variability of black carbon in Athens during wintertime. Air Qual Atmos Heal. 2019;12: 1405-1417.
33. Zhang KM, Allen G, Yang B, Chen G, Gu J, Schwab J, et al. Joint measurements of PM2:5 and light-absorptive PM in woodsmoke-dominated ambient and plume environments. Atmos Chem Phys. 2017;17(18):11441–52.
34. Liu X, Schnelle-Kreis J, Zhang X, Bendl J, Khedr M, Jakobi G, et al. Integration of air pollution data collected by mobile measurement to derive a preliminary spatiotemporal air pollution profile from two neighboring German-Czech border villages. Sci Total Environ. 2020;722:137632.
35. Su JG, Hopke PK, Tian Y, Baldwin N, Thurston SW, Evans K, et al. Modeling particulate matter concentrations measured through mobile monitoring in a deletion/substitution/addition approach. Atmos Environ. 2015;122:477–83.
36. Lightowlers C, Nelson T, Setton E, Peter Keller C. Determining the spatial scale for analysing mobile measurements of air pollution. Atmos Environ. 2008;42(23):5933–7.
37. Reyes R, Schueftan A, Ruiz C, González AD. Controlling air pollution in a context of high energy poverty levels in southern Chile: Clean air but colder houses? Energy Policy. 2019;124: 301-11.
38. Schueftan A, Sommerhoff J, González AD. Firewood demand and energy policy in south-central Chile. Energy Sustain Dev. 2016;33: 26-35.
39. Quinteros ME, Lu S, Blazquez C, Cárdenas-R JP, Ossa X, Delgado-Saborit J-M, et al. Use of data imputation tools to reconstruct incomplete air quality datasets: A case-study in Temuco, Chile. Atmos Environ. 2019 Mar 1;200:40–9.
40. Biblioteca del Congreso Nacional, Chile. Reportes estadísticos comunales 2017.
41. Michael D. Hays, Christopher D. Geron, Kara J. Linna and, Smith* ND, Schauer JJ. Speciation of Gas-Phase and Fine Particle Emissions from Burning of Foliar Fuels. Environ Sci Technol. 2002 Jun 1;36(11):2281–95.
42. Kleeman MJ, Schauer JJ, Cass GR. Size and Composition Distribution of Fine Particulate Matter Emitted from Wood Burning, Meat Charbroiling, and Cigarettes. Environ Sci Technol. 1999;33(20):3516–23.
43. HEI. Understanding the Health Effects of Ambient Ultrafine Particles. Health Effect Institute. 2013.

44. Subdepartamento de Climatología y Meteorología Aplicada. Anuario Meteorológico 2019 Santiago - Chile. 2020;61. Available from: https://climatologia.meteochile.gob.cl/application/publicaciones/anuario/2019
45. Ministerio de Desarrollo Social. Casen 2017: Región de la Araucanía 1 Resumen de resultados Pobreza Multidimensional. 2017;1–12. Available from: http://observatorio.ministeriodesarrollosocial.gob.cl/casen-multidimensional/casen/basedatos.php.
46. Ministerio del Medio Ambiente. Establece plan de descontaminación atmosférica por MP2,5 para las comunas de Temuco y Padre Las Casas actualización del plan de descontaminación por MP10, para las mismas comunas. Decreto 8 2015 [Internet]. Available from: https://mma.gob.cl/wp-content/uploads/2018/07/PDA-Temuco-y-Padre-de-las-Casas-DS-N°8-2015-MMA.pdf
47. Instituto Nacional de Estadística. Anuarios parque de vehículos en circulación. 2017.
48. MINSAL. Diagnósticos regionales en salud con enfoque en determinantes sociales. Ficha regional: Araucanía. 2016.
49. Molina Sepúlveda V OGE. Estudio de la factibilidad de un sistema eficiente de calefacción para la ciudad de Temuco [Internet]. Available from: http//cybertesis.uach.cl/tesis/uach/2013/bpmfem722e/doc/bpmfem722e.pdf. 2013
50. Gómez W, Salgado H, Vásquez F, Chávez C. Using stated preference methods to design cost-effective subsidy programs to induce technology adoption: An application to a stove program in southern Chile. J Environ Manage. 2014;132:346-57.
51. Ministerio del Medio Ambiente. Sistema de Información Nacional de Calidad de Aire: Las Encinas [Internet]. Available from: https://sinca.mma.gob.cl/index.php/estacion/index/id/186
52. Corvalán RM, Osses M, Urrutia CM. Hot emission model for mobile sources: application to the Metropolitan Region of the city of Santiago, Chile. J Air Waste Manag Assoc. 2002;52(2):167–74.
53. Stampfer O, Austin E, Ganuelas T, Fiander T, Seto E, Karr CJ. Use of low-cost PM monitors and a multi-wavelength aethalometer to characterize PM2.5 in the Yakama Nation reservation. Atmos Environ. 2020;224(January):117292.
54. Brunsdon, Chris, Comber L. An Introduction to R for Spatial Analysis and Mapping. Sage Publications; 2015.
55. Carrasco-Escobar G, Schwalb A, Tello-Lizarraga K, Vega-Guerovich P, Ugarte-Gil C. Spatio-temporal co-occurrence of hotspots of tuberculosis, poverty and air pollution in Lima, Peru. Infect Dis Poverty. 2020;9(1):1–6.
56. Instituto Nacional de Estadísticas C. XVII Censo Nacional de Población y VI de Vivienda. 2002.
57. Team Rs. RStudio: Integrated Development for R. Boston, MA: RStudio, Inc.; 2016.
58. Aprueba ley sobre bases generales del medio ambiente [Internet]. [cited 2017 Nov 25]. Available from: https://www.leychile.cl/Navegar?idNorma=30667
59. US Environmental Protection Agency. NAAQS Table. [cited 2017 Apr 28]; Available from: https://www.epa.gov/criteria-air-pollutants/naaqs-table

60. World Health Organization. WHO Air quality guidelines for particulate matter, ozone, nitrogen dioxide and sulfur dioxide: Global update. WHO Air quality guidelines. 2021.
61. Wang Y, Hopke PK, Utell MJ. Urban-scale spatial-temporal variability of black carbon and winter residential wood combustion particles. Aerosol Air Qual Res. 2011;11(5):473–81.
62. Instituto Nacional de Estadísticas C. Resultados CENSO 2017 [Internet]. 2017 [cited 2021 Jan 10]. Available from: http://resultados.censo2017.cl/
63. Kumar P, Morawska L, Birmili W, Paasonen P, Hu M, Kulmala M, et al. Ultrafine particles in cities. Environ Int. 2014;66:1–10.
64. Morawska L, Ristovski Z, Jayaratne ER, Keogh DU, Ling X. Ambient nano and ultrafine particles from motor vehicle emissions: Characteristics, ambient processing and implications on human exposure. Atmos Environ. 2008;42(35):8113–38.
65. Jhun I, Oyola P, Moreno F, Castillo MA, Koutrakis P. PM2.5 mass and species trends in Santiago, Chile, 1998 to 2010: The impact of fuel-related interventions and fuel sales. J Air Waste Manag Assoc. 2013;63(2):161–9.
66. World Air Quality. 2019 World Air Qual Rep [Internet]. 2019;1–22. Available from: https://www.iqair.com/world-most-polluted-cities/world-air-quality-report-2019-en.pdf
67. Ministerio del Medio Ambiente. Guía de calefacción sustentable: Temuco y Padre Las Casas [Internet]. 2018. Available from: http://www.calefaccionsustentable.cl/wp-content/uploads/2018/07/09-calefaccion-sustentable-temuco.pdf

Supplementary Material

Spatial distribution of particulate matter on winter nights in Temuco, Chile: studying the impact of residential wood-burning using mobile monitoring

Estela Blanco[a], Francisco Rubilar[b], Maria Elisa Quinteros[c], Karen Cayupi[b], Salvador Ayala[a], Siyao Lu[d], Raquel B. Jimenez[e], Juan Pablo Cárdenas[b], Carola A. Blazquez[f], Juana Maria Delgado-Saborit[g,h], Roy M. Harrison[g,i], Pablo Ruiz-Rudolph[j*]

[a] Programa de Doctorado en Salud Pública, Instituto de Salud Poblacional, Facultad de Medicina, Universidad de Chile, Independencia 939, Independencia, Santiago, Chile.

[b] Instituto del Medio Ambiente, Universidad de La Frontera, Avenida Francisco Salazar 01145, Temuco, Chile.

[c] Departamento de Salud Pública. Facultad de Ciencias de la Salud, Universidad de Talca, Avenida Lircay s/n, Talca, Chile.

[d] Department of Environmental Health Sciences, University of Michigan, 1415 Washington Heights, Ann Arbor, MI 48109, USA.

[e] Department of Environmental Health, School of Public Health, Boston University, Boston, MA, USA

[f] Department of Engineering Sciences, Universidad Andres Bello, Quillota 980, Viña del Mar, 2531015, Chile.

[g] Division of Environmental Health and Risk Management, School of Geography, Earth and Environmental Sciences, University of Birmingham, Birmingham, UK.

[h] Perinatal Epidemiology, Environmental Health and Clinical Research, School of Medicine, Universitat Jaume I, Avinguda de Vicent Sos Baynat, s/n, 12071 Castelló de la Plana, Castellon, Spain.

[i] Department of Environmental Sciences / Center of Excellence in Environmental Studies, King Abdulaziz University, PO Box 80203, Jeddah, 21589, Saudi Arabia.

[j] Programa de Salud Ambiental, Instituto de Salud Poblacional, Facultad de Medicina, Universidad de Chile, Independencia 939, Independencia, Santiago, Chile.

[*]Corresponding author

Corresponding Author

Pablo Ruiz-Rudolph. Programa de Salud Ambiental, Instituto de Salud Poblacional, Facultad de Medicina, Universidad de Chile, Independencia 939, Independencia, Santiago, Chile; pabloruizr@uchile.cl; phone (+56-22-978-6379)

Details on application of correction factors to portable instruments

It is known that Dust-Trak instruments actually measures volume which then is expressed as concentrations assuming certain density and that the sensitivity of measurements tend to drift over time. This later point can apply to P-TRAKs also. Dust-Trak come from manufacturer using a density of 2.5 mg/mL which is close to soil dust so to be applied to occupational exposures (for instance, dust from drilling). In order to make Dust-Trak measurements more comparable to government measurements, data collected with the Dust-Trak at the central site (during 6 hours) was compared with government data and a correction factor was derived for each our and then averaged. This correction was then applied to both Dust-Trak measurements. We prefer to derive a daily correction factor as the instrument might drift from day to day.

Additionally, as instruments sensitivity might drift from day to day, a second correction was applied to both mobile Dust-Trak and P-TRAK using the initial and final 3-minute collocated data with the central site ones. A daily correction factor was derived averaging initial and final corrections factors.

This way, we assure measurements of the Dust-Trak at central site are comparable to government measurements while mobile Dust-Trak are comparable to both central site Dust-Trak and government measurements.

Table S 1. Daily correction factors (CF) for instruments comparisons.

Date	Route	P-TRAK Duplicates CF	DT Duplicates CF	DT-Government CF
5/26/2016	Labranza	0.706	1.01	212.5
6/8/2016	Amanecer		0.996	219
6/14/2016	Amanecer	0.88	0.966	247.9
6/16/2016	Las Encinas	0.752	0.995	442
6/20/2016	Pedro de Valdivia	0.63	0.954	201
6/21/2016	Padre las Casas	0.688	1.002	215.6
6/28/2016	Labranza	0.794	0.983	238.8
6/29/2016	Labranza	0.762	1.007	212
6/30/2016	Las Encinas	0.725	1.025	277.2
7/1/2016	Pedro de Valdivia	0.685	0.998	224.1
7/4/2016	Amanecer	0.785	0.974	158.5

7/5/2016	Padre las Casas	0.768	0.973	234.1
7/6/2016	Las Encinas	0.788	1.000	218
7/7/2016	Labranza	0.767	0.995	178.5
7/8/2016	Pedro de Valdivia	0.81	0.977	292.8
7/11/2016	Padre las Casas	0.734	0.996	289
7/12/2016	Amanecer	0.733	0.928	316
7/13/2016	Las Encinas	0.764	0.986	450.5
7/14/2016	Pedro de Valdivia	0.767	0.998	250.6
7/15/2016	Padre las Casas	0.758	1.004	235.2
	Median	**0.762**	**0.996**	**235**
	p25%	**0.729**	**0.976**	**215**
	p75%	**0.777**	**1.001**	**280**

Table S 2. Description of monitoring sessions.

Date	Route	Weather conditions	Comments
5/26/16	Labranza	Clear	
6/08/16	Amanecer	Clear	UFP central site data losses
6/14/16	Amanecer	Clear	
6/16/16	Las Encinas	Clear	
6/20/16	Pedro de Valdivia	Foggy	Mobile UFP data losses
6/21/16	Padre las Casas	Foggy	Central site data losses
6/28/16	Labranza	Foggy	
6/29/16	Labranza	Rain	
6/30/16	Las Encinas	Clear	
7/1/16	Pedro de Valdivia	Foggy	
7/4/16	Amanecer	Foggy	
7/5/16	Padre las Casas	Foggy	

7/6/16	Las Encinas	Clear	
7/7/16	Labranza	Clear	
7/8/16	Pedro de Valdivia	Rain	
7/11/16	Padre Las Casas	Clear	Incomplete routes Central site data losses
7/12/16	Amanecer	Rain	
7/13/16	Las Encinas	Rain	
7/14/16	Pedro de Valdivia	Rain	
7/15/16	Padre Las Casas	Rain	

Table S 3. Central site summary statistics by route.

	Variable											
	$PM_{2.5}$ (µg m-3)			Temperature (°C)			Relative Humidity (%)			Wind Speed (m/s)		
Route	**N***	**Mean**	**SD**	**N**	**Mean**	**SD**	**N**	**Mean**	**SD**	**N**	**Mean**	**SD**
Amanecer	24	135.8	152.2	24	7.8	2.1	23	96.1	5.0	24	0.8	0.7
Labranza	24	161.7	80.1	24	8.1	1.5	12	94.8	6.1	23	0.5	0.4
Las Encinas	24	128.3	137.7	24	7.8	1.7	24	97.6	3.6	24	1.1	0.9
Padre las Casas	24	133.6	146.4	24	7.3	1.7	21	88.9	7.9	23	1.2	0.9
Pedro de Valdivia	24	117.4	101.6	24	7.4	2.2	23	92.8	5.6	24	0.9	0.6

*Hourly observations

Table S 4a. Summary statistics for $PM_{2.5}$ concentrations for mobile pollutant measurements summarized by day within 200m cell raster, with mean values of selected variables recorded at government central site.

		Mobile Measurements (µg m-3)								Central Site					
Date	**Route**	**N obs**	**Mean**	**SD**	**p5%**	**p25%**	**Median**	**p75%**	**p95%**	**$PM_{2.5}$ (µg m-3) Mean**	**Temp. (°C) Mean**	**HR (%) Mean**	**PP (mm/h) Mean**	**Wind Speed (ms) Mean**	**Wind Dir.**
2016-06-08	Amanecer	185	83.7	48.2	20.1	45.3	76.8	116.1	174.9	66.1	9.7	95.4	0.9	0.7	E
2016-06-14	Amanecer	343	48.2	30.3	14.5	24.9	38.4	66.7	107.8	35.7	7.9	100.0	0.0	0.8	SE
2016-07-04	Amanecer	244	124.1	112.6	40.3	55.2	77.5	140.9	398.4	350.6	4.6	98.9	0.0	0.1	E
2016-07-12	Amanecer	113	110.0	39.0	57.7	76.7	102.6	140.7	174.7	90.9	9.2	90.0	0.0	1.4	E
2016-05-26	Labranza	330	137.0	108.9	14.0	71.2	108.9	187.0	342.1	167.5	10.2	90.8	0.0	0.3	E
2016-06-28	Labranza	323	87.4	49.7	23.4	49.6	80.1	111.5	190.4	110.7	6.9		0.0	0.9	E
2016-06-29	Labranza	241	133.6	139.1	29.1	51.2	81.6	163.7	391.5	174.4	7.2		0.0	0.3	W
2016-07-07	Labranza	373	119.7	68.3	35.4	67.7	102.7	159.8	242.7	194.2	8.1	98.7	0.0	0.6	NE
2016-06-16	Las Encinas	215	382.2	264.1	55.6	170.6	311.1	590.9	862.3	292.5	7.2	96.7	0.0	0.3	W
2016-06-30	Las Encinas	191	202.5	146.3	59.6	115.4	151.2	232.6	512.6	152.1	6.0	94.8	0.0	0.4	NE
2016-07-06	Las Encinas	201	52.1	21.7	22.2	33.6	51.1	67.0	92.8	29.1	9.9	98.9	0.1	1.5	E
2016-07-13	Las Encinas	204	34.9	21.8	13.5	20.1	27.5	43.2	81.5	39.6	8.1	100.0	1.4	2.1	W

		Mobile Measurements (µg m-3)								Central Site					
Date	Route	N obs	Mean	SD	p5%	p25%	Median	p75%	p95%	$PM_{2.5}$ (µg m-3) Mean	Temp. (°C) Mean	HR (%) Mean	PP (mm/h) Mean	Wind Speed (ms) Mean	Wind Dir.
2016-06-21	Padre las Casas	116	198.9	104.9	66.2	138.6	171.2	246.7	371.8	307.3	5.2	98.7	0.0	0.4	E
2016-07-05	Padre las Casas	156	41.3	19.2	14.8	28.7	37.1	50.8	82.5	81.2	7.8	79.4	0.0	0.8	E
2016-07-11	Padre las Casas	150	43.0	21.8	13.8	25.4	38.6	60.0	80.3	50.7	9.6	86.3	0.1	2.2	S
2016-07-15	Padre las Casas	167	100.7	47.9	38.6	59.8	90.9	141.8	188.9	95.2	6.6	96.0	0.0	1.1	E
2016-06-20	P. de Valdivia	250	133.0	89.6	28.6	61.9	112.9	181.5	306.7	158.8	6.8	93.9	0.0	0.3	SE
2016-07-01	P. de Valdivia	232	235.2	136.0	65.7	133.9	207.3	319.0	499.9	183.9	5.5	95.1	0.0	0.8	NE
2016-07-08	P. de Valdivia	231	36.4	18.6	10.5	21.4	34.6	49.4	71.4	50.3	10.6	89.4	0.4	1.5	SE
2016-07-14	P. de Valdivia	212	58.3	37.6	20.6	29.0	50.8	71.6	137.4	76.6	6.9	92.9	0.0	1.1	E

PP: precipitations. P. de Valdivia: Pedro de Valdivia

Table S 4b. Summary statistics for $PM_{2.5}$ ratios for mobile pollutant measurements summarized by day within 200m cell raster, with mean values of selected variables recorded at government central site.

		Mobile Measurements (µg m-3)								Central Site					
Date	**Route**	**N obs**	**Mean**	**SD**	**p5%**	**p25%**	**Median**	**p75%**	**p95%**	**$PM_{2.5}$ (µg m-3) Mean**	**Temp. (°C) Mean**	**HR (%) Mean**	**PP (mm/h) Mean**	**Wind Speed (ms) Mean**	**Wind Dir.**
2016-06-08	Amanecer	185	1.6	0.9	0.5	0.9	1.4	2.2	3.2	56.0	9.4	96.7	0.9	0.7	E
2016-06-14	Amanecer	343	1.3	0.7	0.3	0.7	1.1	1.7	2.6	26.6	7.8	100.0	0.0	0.8	SE
2016-07-04	Amanecer	244	0.4	0.4	0.1	0.1	0.2	0.5	1.4	292.1	4.2	99.0	0.0	0.2	E
2016-07-12	Amanecer	113	1.0	0.4	0.5	0.7	0.9	1.4	1.8	40.5	9.0	90.2	0.1	1.6	E
2016-05-26	Labranza	330	0.7	0.6	0.1	0.3	0.6	0.9	2.2	171.2	9.6	94.0	0.0	0.2	NE
2016-06-28	Labranza	323	0.8	0.5	0.2	0.4	0.7	1.0	1.8	91.1	6.9		0.0	1.1	E
2016-06-29	Labranza	241	0.7	0.5	0.2	0.4	0.6	0.9	1.4	123.0	6.8		0.0	0.3	W
2016-07-07	Labranza	373	0.7	0.5	0.2	0.4	0.6	0.9	1.7	174.7	7.8	99.2	0.0	0.6	NE
2016-06-16	Las Encinas	215	1.9	1.2	0.6	1.1	1.5	2.3	4.7	317.9	6.7	98.1	0.0	0.2	W
2016-06-30	Las Encinas	191	1.1	0.7	0.3	0.6	1.0	1.5	2.5	149.7	5.3	96.0	0.0	0.5	E
2016-07-06	Las Encinas	201	1.6	0.6	0.9	1.2	1.5	2.0	2.6	24.9	9.8	99.0	0.1	1.4	E
2016-07-13	Las Encinas	204	0.8	0.6	0.2	0.4	0.7	1.0	2.1	31.7	8.1	100.0	0.8	2.1	W
2016-06-21	Padre las Casas	47	0.7	0.3	0.3	0.5	0.8	0.9	1.2	224.1	4.9	99.5	0.0	0.5	NE
2016-07-05	Padre las Casas	156	0.5	0.2	0.2	0.3	0.4	0.6	0.8	67.3	7.6	80.5	0.0	0.9	E

		Mobile Measurements (µg m-3)								Central Site					
Date	Route	N obs	Mean	SD	p5%	p25%	Median	p75%	p95%	$PM_{2.5}$ (µg m-3) Mean	Temp. (°C) Mean	HR (%) Mean	PP (mm/h) Mean	Wind Speed (ms) Mean	Wind Dir.
2016-07-11	Padre las Casas	150	0.8	0.5	0.1	0.4	0.7	1.1	1.9	45.0	9.5	85.7	0.1	2.5	S
2016-07-15	Padre las Casas	167	1.0	0.6	0.4	0.6	0.9	1.2	2.1	70.5	6.2	97.6	0.0	1.2	E
2016-06-20	P. de Valdivia	250	0.6	0.4	0.1	0.3	0.5	0.8	1.4	152.1	6.2	96.0	0.0	0.3	SE
2016-07-01	P. de Valdivia	232	1.2	0.6	0.4	0.8	1.0	1.5	2.2	133.9	4.9	97.3	0.0	0.8	NE
2016-07-08	P. de Valdivia	231	1.1	0.6	0.3	0.6	1.1	1.4	2.0	55.6	10.4	91.7	0.4	1.2	SE
2016-07-14	P. de Valdivia	212	0.8	0.5	0.2	0.4	0.7	1.2	1.8	59.7	6.7	93.5	0.0	1.1	E

PP: precipitations. P. de Valdivia: Pedro de Valdivia

Table S 4c. Summary statistics for UFP concentrations for mobile pollutant measurements summarized by day within 200m cell raster, with mean values of selected variables recorded at central government site.

		Mobile Measurements (µg m-3)								Central Site					
Date	**Route**	**N obs**	**Mean**	**SD**	**p5%**	**p25%**	**Median**	**p75%**	**p95%**	**$PM_{2.5}$ (µg m-3) Mean**	**Temp. (°C) Mean**	**HR (%) Mean**	**PP (mm/h) Mean**	**Wind Speed (ms) Mean**	**Wind Dir.**
2016-06-08	Amanecer	0	NA	NA	NA	NA	NA	NA	NA	56.0	9.4	96.7	0.9	0.7	E
2016-06-14	Amanecer	343	26,622.4	20,257.1	6,586.5	14,056.1	20,497.4	33,572.0	63,459.6	26.6	7.8	100.0	0.0	0.8	SE
2016-07-04	Amanecer	244	42,142.6	28,527.1	17,153.2	22,942.5	29,740.7	53,822.2	104,064.9	292.1	4.2	99.0	0.0	0.2	E
2016-07-12	Amanecer	311	20,172.1	12,323.6	5,226.7	10,140.9	18,335.4	28,729.2	40,892.7	40.5	9.0	90.2	0.1	1.6	E
2016-05-26	Labranza	330	52,874.8	27,622.3	20,524.6	32,063.2	47,421.2	65,379.4	111,706.0	171.2	9.6	94.0	0.0	0.2	NE
2016-06-28	Labranza	323	34,000.0	25,781.7	7,398.4	16,271.0	24,312.4	44,624.9	92,727.3	91.1	6.9		0.0	1.1	E
2016-06-29	Labranza	241	57,606.4	27,215.1	18,868.2	35,634.3	55,748.3	74,856.3	103,491.7	123.0	6.8		0.0	0.3	W
2016-07-07	Labranza	373	54,280.0	24,587.3	20,156.4	33,910.5	53,769.0	67,934.5	101,245.8	174.7	7.8	99.2	0.0	0.6	NE
2016-06-16	Las Encinas	215	47,139.4	17,978.1	18,395.9	33,801.1	46,768.0	60,562.6	73,561.5	317.9	6.7	98.1	0.0	0.2	W
2016-06-30	Las Encinas	191	41,869.2	15,208.3	21,941.2	31,626.9	39,730.0	49,366.2	68,596.5	149.7	5.3	96.0	0.0	0.5	E
2016-07-06	Las Encinas	201	20,162.8	8,383.9	9,020.3	13,980.9	19,778.0	24,752.3	30,337.1	24.9	9.8	99.0	0.1	1.4	E
2016-07-13	Las Encinas	204	9,542.2	6,158.1	3,897.5	5,680.3	7,400.8	11,735.7	20,914.8	31.7	8.1	100.0	0.8	2.1	W

		Mobile Measurements (µg m-3)								Central Site					
Date	Route	N obs	Mean	SD	p5%	p25%	Median	p75%	p95%	$PM_{2.5}$ (µg m-3) Mean	Temp. (°C) Mean	HR (%) Mean	PP (mm/h) Mean	Wind Speed (ms) Mean	Wind Dir.
2016-06-21	Padre las Casas	116	43,416.3	18,577.8	14,841.0	29,782.3	41,523.4	52,891.0	77,730.8	224.1	4.9	99.5	0.0	0.5	NE
2016-07-05	Padre las Casas	156	22,016.0	11,505.8	8,621.0	14,294.5	19,233.3	28,129.0	46,710.0	67.3	7.6	80.5	0.0	0.9	E
2016-07-11	Padre las Casas	161	20,640.5	11,689.0	6,734.5	13,877.9	18,672.3	24,047.7	41,136.1	45.0	9.5	85.7	0.1	2.5	S
2016-07-15	Padre las Casas	165	37,617.0	17,703.9	16,879.0	23,369.0	34,808.8	46,544.7	70,745.8	70.5	6.2	97.6	0.0	1.2	E
2016-06-20	P. de Valdivia	166	36,921.0	21,209.1	8,604.1	19,702.5	32,663.9	51,965.9	69,999.7	152.1	6.2	96.0	0.0	0.3	SE
2016-07-01	P. de Valdivia	232	57,435.5	23,884.5	21,000.0	38,807.3	54,961.3	76,589.5	93,071.6	133.9	4.9	97.3	0.0	0.8	NE
2016-07-08	P. de Valdivia	231	13,457.1	9,432.3	4,649.1	8,096.6	11,640.8	16,700.2	26,833.3	55.6	10.4	91.7	0.4	1.2	SE
2016-07-14	P. de Valdivia	212	23,752.9	13,567.0	9,016.4	13,031.9	20,216.4	32,433.6	53,610.9	59.7	6.7	93.5	0.0	1.1	E

PP: precipitations. P. de Valdivia: Pedro de Valdivia

Table S 4d. Summary statistics for UFP ratio for mobile pollutant measurements summarized by day within 200m cell raster, with mean values of selected variables recorded at government central site.

		Mobile Measurements (µg m-3)								Central Site					
Date	**Route**	**N obs**	**Mean**	**SD**	**p5%**	**p25%**	**Median**	**p75%**	**p95%**	**$PM_{2.5}$ (µg m-3) Mean**	**Temp. (°C) Mean**	**HR (%) Mean**	**PP (mm/h) Mean**	**Wind Speed (ms) Mean**	**Wind Dir.**
2016-06-08	Amanecer	0	NA	NA	NA	NA	NA	NA	NA	56.0	9.4	96.7	0.9	0.7	E
2016-06-14	Amanecer	343	2.3	1.7	0.6	1.3	1.9	2.9	5.4	26.6	7.8	100.0	0.0	0.8	SE
2016-07-04	Amanecer	244	0.7	0.5	0.3	0.4	0.6	0.9	1.8	292.1	4.2	99.0	0.0	0.2	E
2016-07-12	Amanecer	311	1.3	0.6	0.6	0.9	1.2	1.6	2.3	40.5	9.0	90.2	0.1	1.6	E
2016-05-26	Labranza	330	1.4	0.8	0.5	0.9	1.2	1.8	3.0	171.2	9.6	94.0	0.0	0.2	NE
2016-06-28	Labranza	323	1.3	1.0	0.3	0.6	1.1	1.8	3.3	91.1	6.9		0.0	1.1	E
2016-06-29	Labranza	241	1.9	1.0	0.8	1.3	1.7	2.4	3.8	123.0	6.8		0.0	0.3	W
2016-07-07	Labranza	373	1.6	0.8	0.7	0.9	1.3	2.0	3.1	174.7	7.8	99.2	0.0	0.6	NE
2016-06-16	Las Encinas	215	1.6	0.7	0.9	1.2	1.5	1.9	2.9	317.9	6.7	98.1	0.0	0.2	W
2016-06-30	Las Encinas	191	1.2	0.4	0.6	0.9	1.1	1.5	1.9	149.7	5.3	96.0	0.0	0.5	E
2016-07-06	Las Encinas	201	1.6	0.5	1.0	1.2	1.5	1.9	2.3	24.9	9.8	99.0	0.1	1.4	E
2016-07-13	Las Encinas	204	1.1	0.7	0.3	0.6	1.0	1.4	2.4	31.7	8.1	100.0	0.8	2.1	W

		Mobile Measurements (µg m-3)								Central Site					
Date	Route	N obs	Mean	SD	p5%	p25%	Median	p75%	p95%	$PM_{2.5}$ (µg m-3) Mean	Temp. (°C) Mean	HR (%) Mean	PP (mm/h) Mean	Wind Speed (ms) Mean	Wind Dir.
2016-06-21	Padre las Casas	116	1.2	0.5	0.6	0.8	1.1	1.6	2.0	224.1	4.9	99.5	0.0	0.5	NE
2016-07-05	Padre las Casas	156	0.9	0.6	0.3	0.5	0.8	1.0	2.2	67.3	7.6	80.5	0.0	0.9	E
2016-07-11	Padre las Casas	161	1.2	0.7	0.3	0.7	1.0	1.4	2.6	45.0	9.5	85.7	0.1	2.5	S
2016-07-15	Padre las Casas	165	1.4	0.8	0.6	1.0	1.3	1.7	2.4	70.5	6.2	97.6	0.0	1.2	E
2016-06-20	P. de Valdivia	166	0.9	0.5	0.2	0.6	0.8	1.0	1.7	152.1	6.2	96.0	0.0	0.3	SE
2016-07-01	P. de Valdivia	232	1.4	0.5	0.6	1.1	1.3	1.6	2.2	133.9	4.9	97.3	0.0	0.8	NE
2016-07-08	P. de Valdivia	231	1.7	1.5	0.5	0.9	1.4	2.0	3.7	55.6	10.4	91.7	0.4	1.2	SE
2016-07-14	P. de Valdivia	212	1.1	0.6	0.4	0.6	1.0	1.6	2.4	59.7	6.7	93.5	0.0	1.1	E

PP: precipitations. P. de Valdivia: Pedro de Valdivia

Table S 5. Percent of neighborhood categorized as hot and cold spot, according to Local Moran

	Hot Spots		Cold Spots	
	$PM_{2.5}$	UFP	$PM_{2.5}$	UFP
5 DE ABRIL	0.0	**21.6**	**21.6**	0.0
ALIANZA	0.0	0.0	**68.8**	**43.8**
AMANECER	**69.4**	**46.9**	0.0	0.0
BALMACEDA	0.0	0.0	0.0	0.0
CAMPOS DEPORTIVOS	**33.3**	**44.4**	0.0	0.0
CAUPOLICAN	0.0	0.0	8.3	0.0
CENTRAL	0.0	0.0	0.0	0.0
DREVES	0.0	**22.2**	0.0	0.0
ERNESTO BOHN	**25.0**	**88.9**	0.0	0.0
ESTACION	0.0	**50.0**	0.0	0.0
ESTADIO	0.0	0.0	0.0	0.0
EVARISTO MARIN	**75.0**	**55.6**	0.0	0.0
IGUALDAD Y TRABAJO	**50.0**	7.1	0.0	0.0
IMPERIAL	0.0	**25.0**	0.0	0.0
JOSE MIGUEL CARRERA	**54.1**	0.0	0.0	0.0
LA UNION	0.0	0.0	**85.7**	**37.5**
LABRANZA	5.9	0.0	7.4	**26.5**
LAS HERAS	0.0	9.1	0.0	0.0
LAS QUILAS	0.0	6.7	0.0	0.0

LOS JARDINES	0.0	0.0	**44.4**	0.0
LOS LAURELES	0.0	**66.7**	0.0	0.0
LOURDES	0.0	**33.3**	0.0	0.0
MAESTRANZA	**75.0**	**84.6**	0.0	0.0
MAQUEHUE	0.0	0.0	5.9	0.0
MILLARAY	**75.0**	**25.0**	0.0	0.0
NIELOL	0.0	0.0	0.0	0.0
PAREDES	**22.2**	**22.2**	0.0	0.0
PEDRO DE VALDIVIA	0.0	0.0	**54.5**	**27.3**
PICHI CAUTIN	0.0	0.0	0.0	0.0
POMONA	**42.9**	**28.6**	0.0	0.0
PORVENIR	15.6	**25.0**	18.8	0.0
RIBERENOS	0.0	0.0	**36.8**	5.0
SAN ANTONIO	0.0	0.0	3.7	0.0
SANTA ROSA	11.1	0.0	0.0	0.0
SOFO	0.0	0.0	4.3	0.0
THIERS	0.0	0.0	3.0	0.0
TROMEN	12.0	**27.8**	4.8	0.0
TROMEN MOLULCO	5.6	0	16.7	15.0
TUCAPEL	**20.0**	**100.0**	0.0	0.0
UNIVERSIDAD	**46.9**	**20.3**	0.0	0.0
VILLA ALEGRE	0.0	0.0	**100.0**	0.0
VILLA SUR	**30.0**	**30.0**	0.0	0.0

VILLA TURINGIA	**25.6**	4.7	0.0	4.7
VISTA HERMOSA	0.0	5.9	14.7	11.8

Figure S 1. Inlet tubing connected to outside air through car window used for mobile measurements.

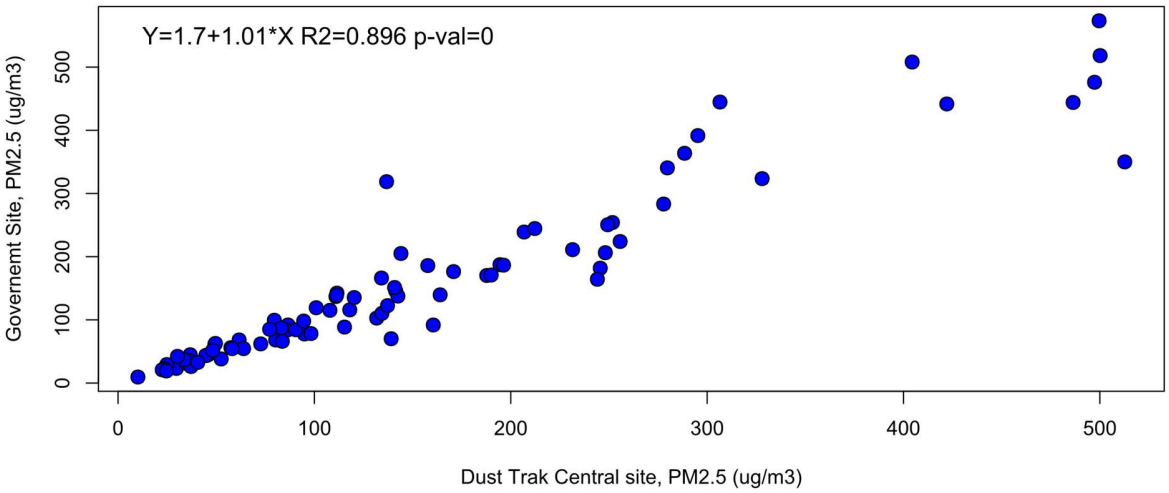

Figure S 2. Comparison of hourly PM2.5 means recorded at the government central site versus DustTrak central site.

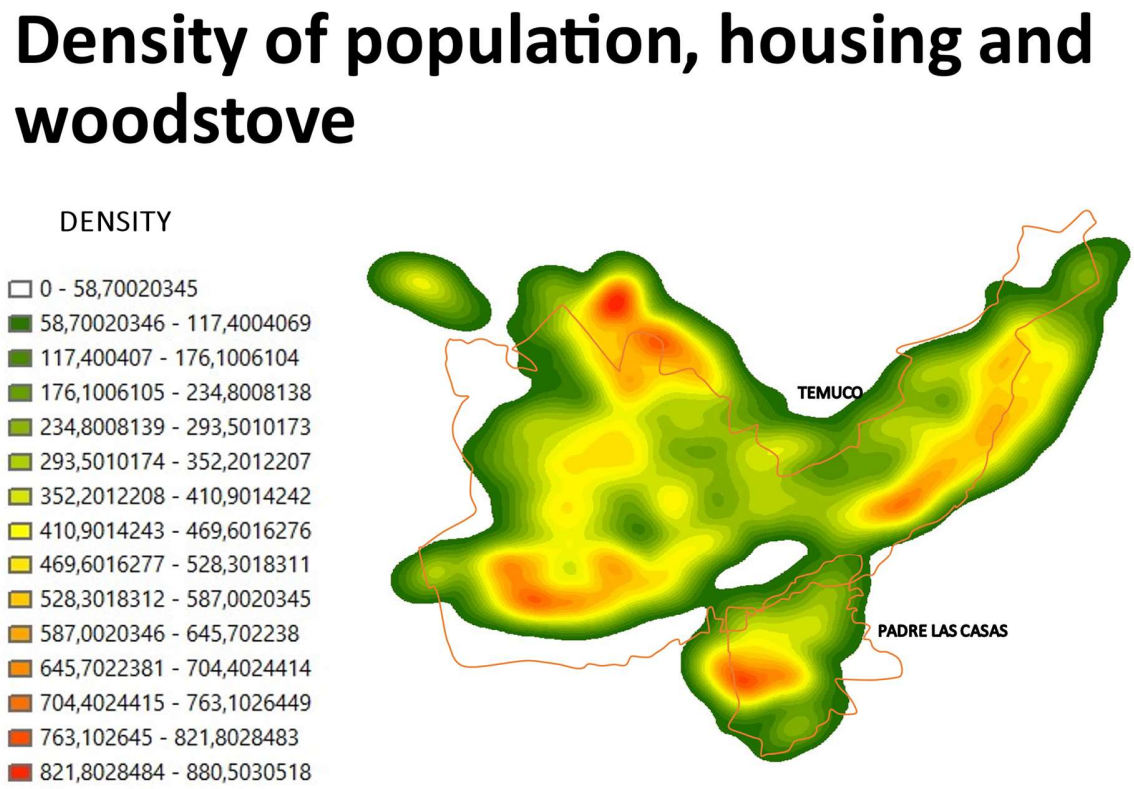

Figure S 3. Kernel of predictors used to design sampling routes.

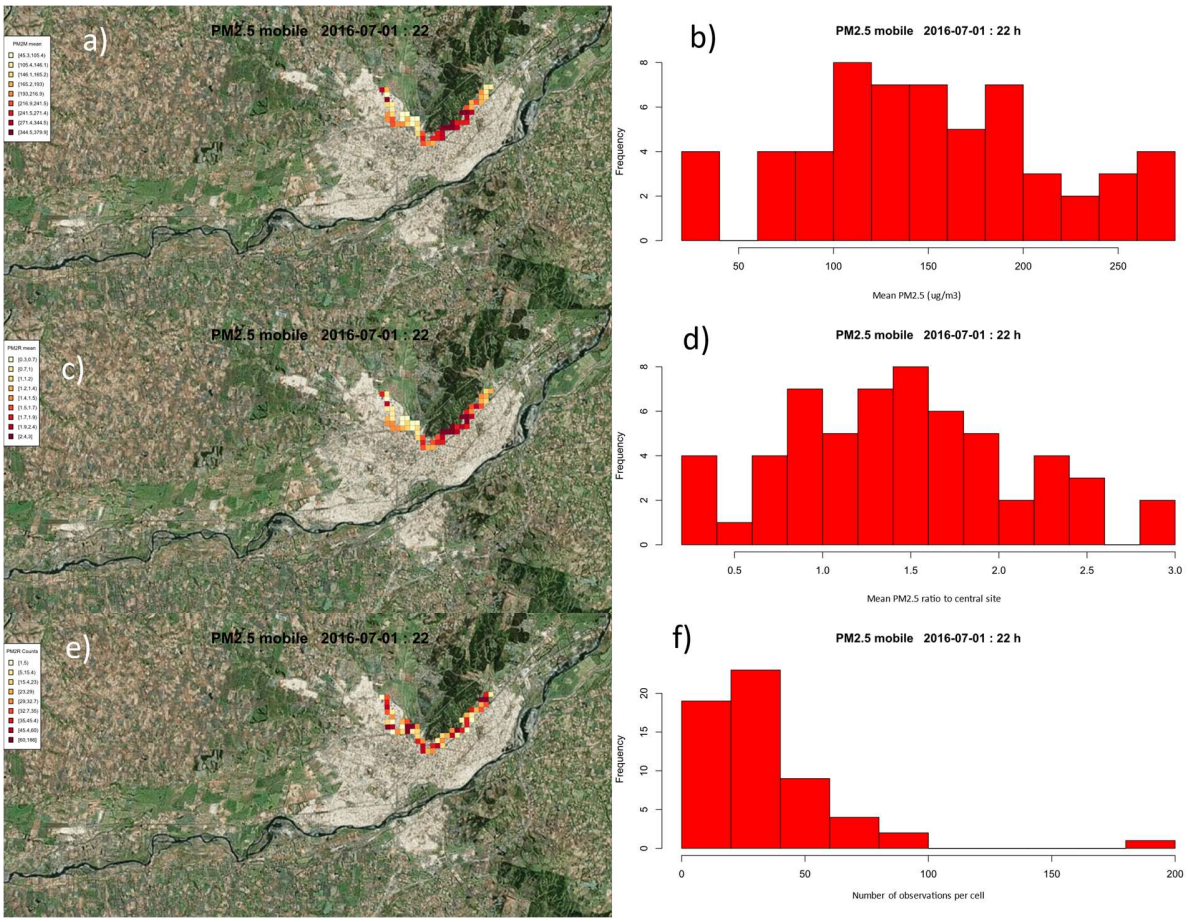

Figure S 4a. Examples of collapse by the mean for a raster of 200m cell for given hour (7/1/2016 21:00). a) Plot of mean $PM_{2.5}$ concentrations, b) histogram of mean $PM_{2.5}$ concentrations, c) plot of mean $PM_{2.5}$ ratios, d) histogram of mean $PM_{2.5}$ concentrations

in each cell for the hourly raster, e) plot of counts (number of observations), f) histogram plot of counts (number of observations).

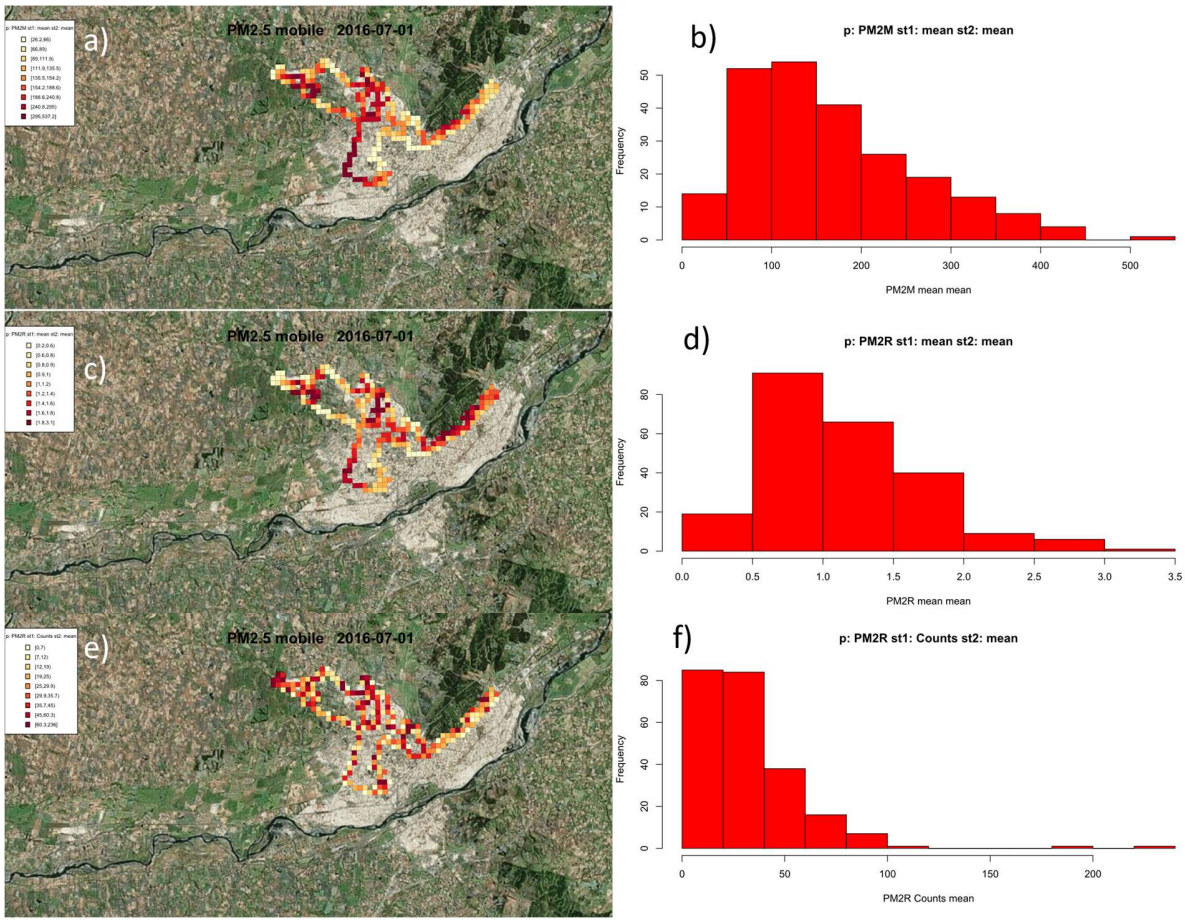

Figure S 4b. Examples of collapse by the mean for a raster of 200m cell for a given day (7/1/2016). a) Plot of mean $PM_{2.5}$ concentrations, b) histogram of mean $PM_{2.5}$ concentrations, c) plot of mean $PM_{2.5}$ ratios, d) histogram of mean $PM_{2.5}$ concentrations in each cell for the hourly raster, e) plot of counts (number of observations), f) histogram plot of counts (number of observations).

63

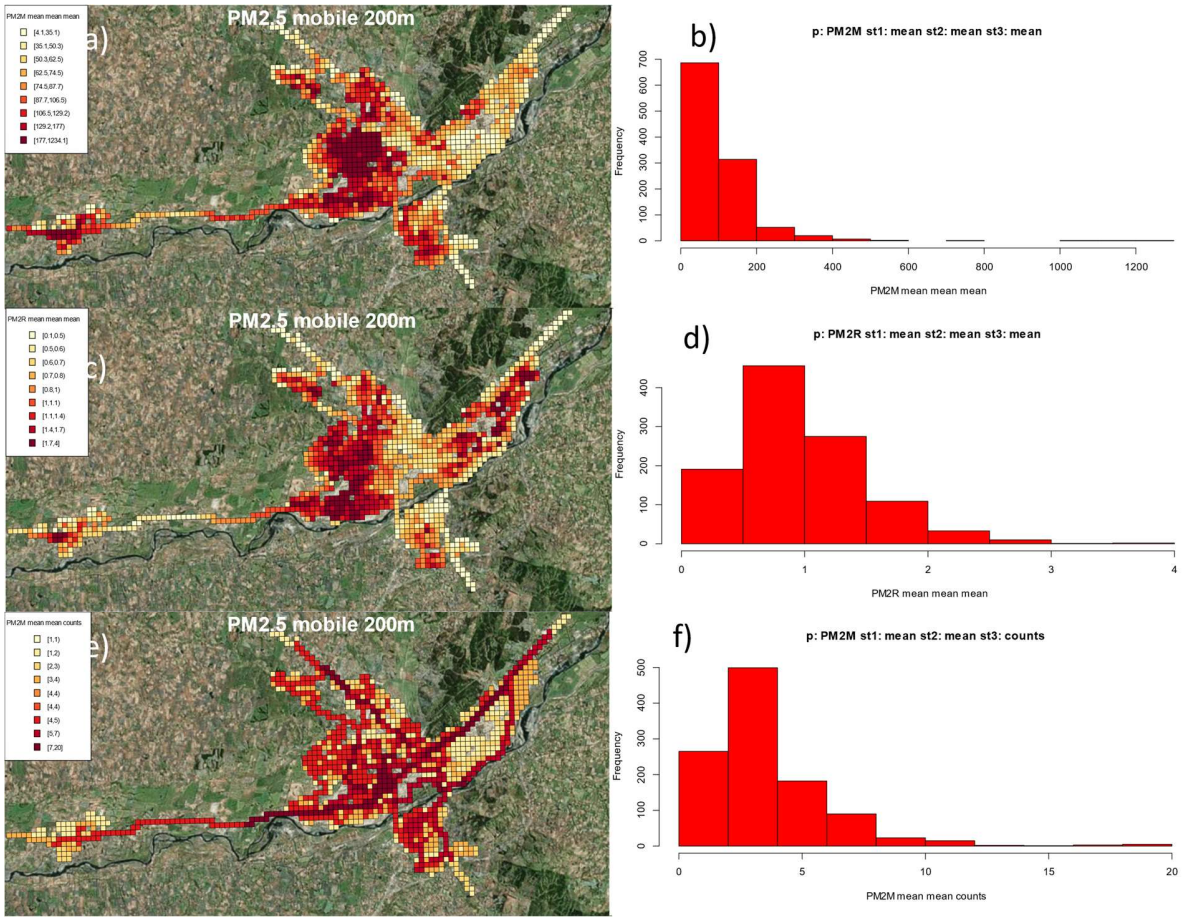

Figure S 4c. Examples of collapse for a raster of 200m cell for the 20 days) Plot of mean $PM_{2.5}$ concentrations, b) histogram of mean $PM_{2.5}$ concentrations, c) plot of mean $PM_{2.5}$ ratios, d) histogram of mean $PM_{2.5}$ concentrations in each cell for the hourly raster, e)

plot of counts (number of days with observations per cell), f) histogram plot of counts (number of days with observations per cell).

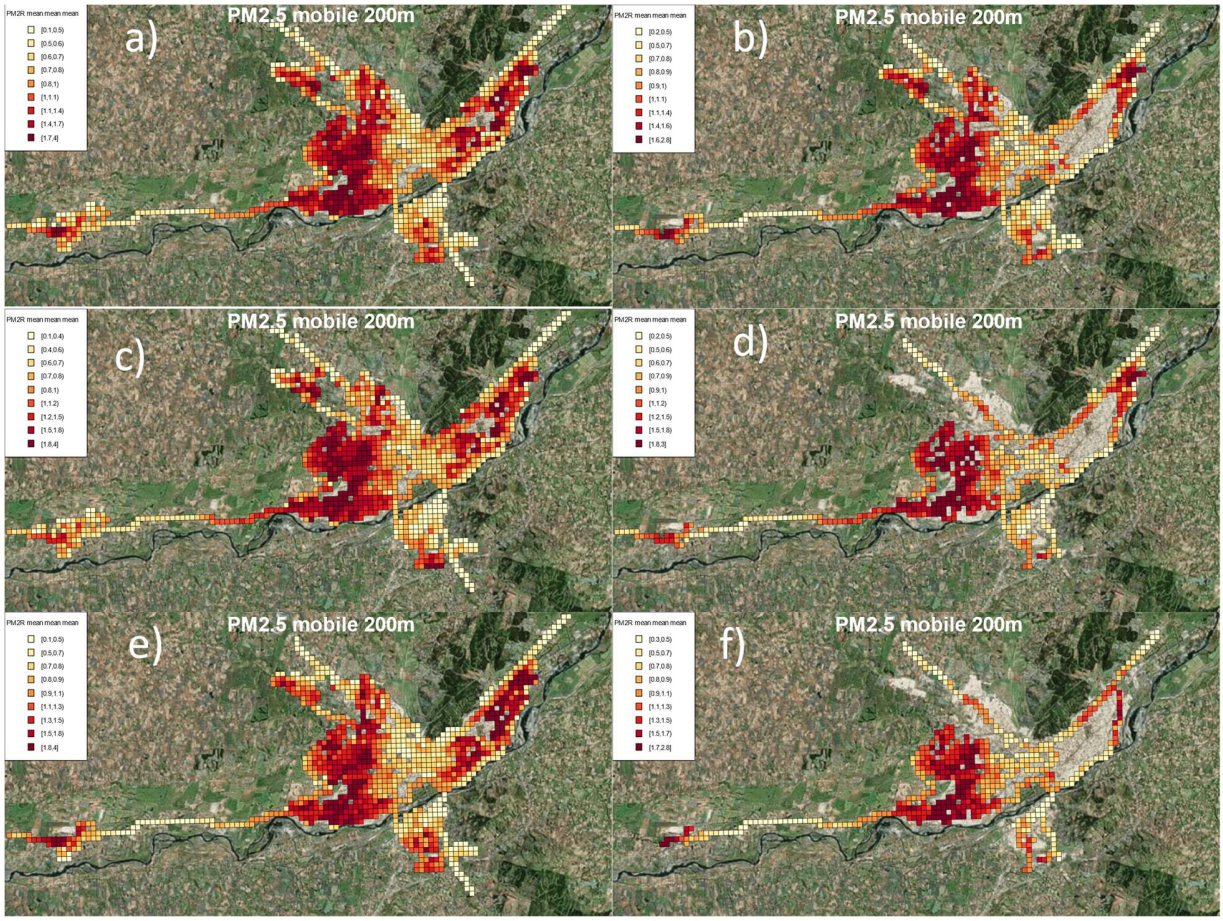

Figure S 5a. Sensitivity plots. Plots of ratios of $PM_{2.5}$ for 200-m cell rasters, for a) all data, b) excluding cells with less than 3 observations per cell when collapsing each hour and cells with less than 3 days of observations when collapsing all days, c) excluding days of rain, d) excluding days with rain and excluding cells with less than 3 observations per cell when collapsing each hour and cells with less than 3 days of observations when collapsing all days, e) excluding days of fog, f) excluding days with fog and excluding cells with less than 3 observations per cell when collapsing each hour and cells with less than 3 days of observations when collapsing all days.

90

91

92

93

94

95

96

97

98

99

100

101

102

103

104

105

106

107

108

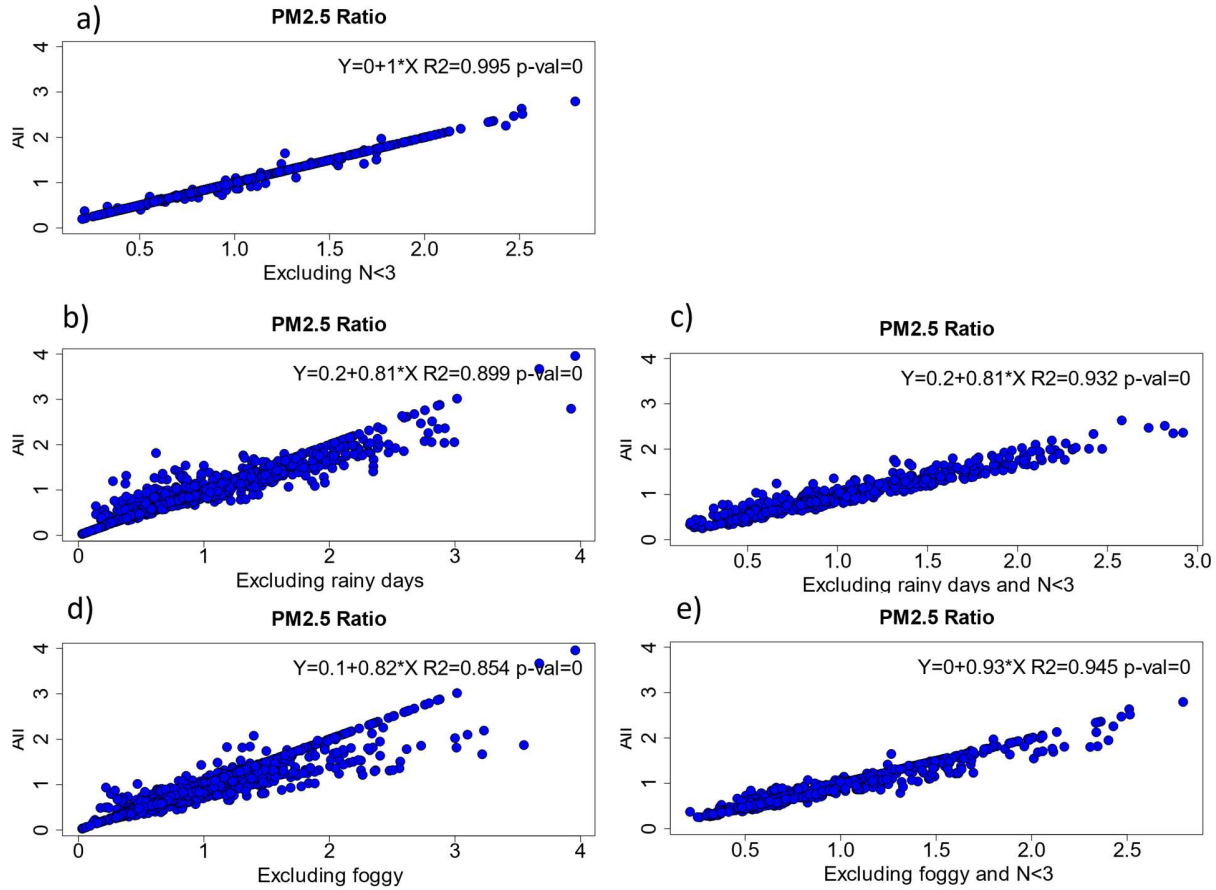

Figure S 5b. Comparison plots for sensitivity analyses. Plots of ratios of $PM_{2.5}$ for 200-m cell rasters comparing a) all data vs excluding cells with less than 3 observations per cell when collapsing each hour and cells with less than 3 days of observations when collapsing all days, b) all data vs. excluding days of rain, c) all data vs. excluding days with rain and excluding cells with less than 3 observations per cell when collapsing each hour and cells with less than 3 days of observations when collapsing all days, d) all data vs. excluding days of fog, e) all data vs. excluding days with fog and excluding cells with less than 3 observations per cell when collapsing each hour and cells with less than 3 days of observations when collapsing all days.

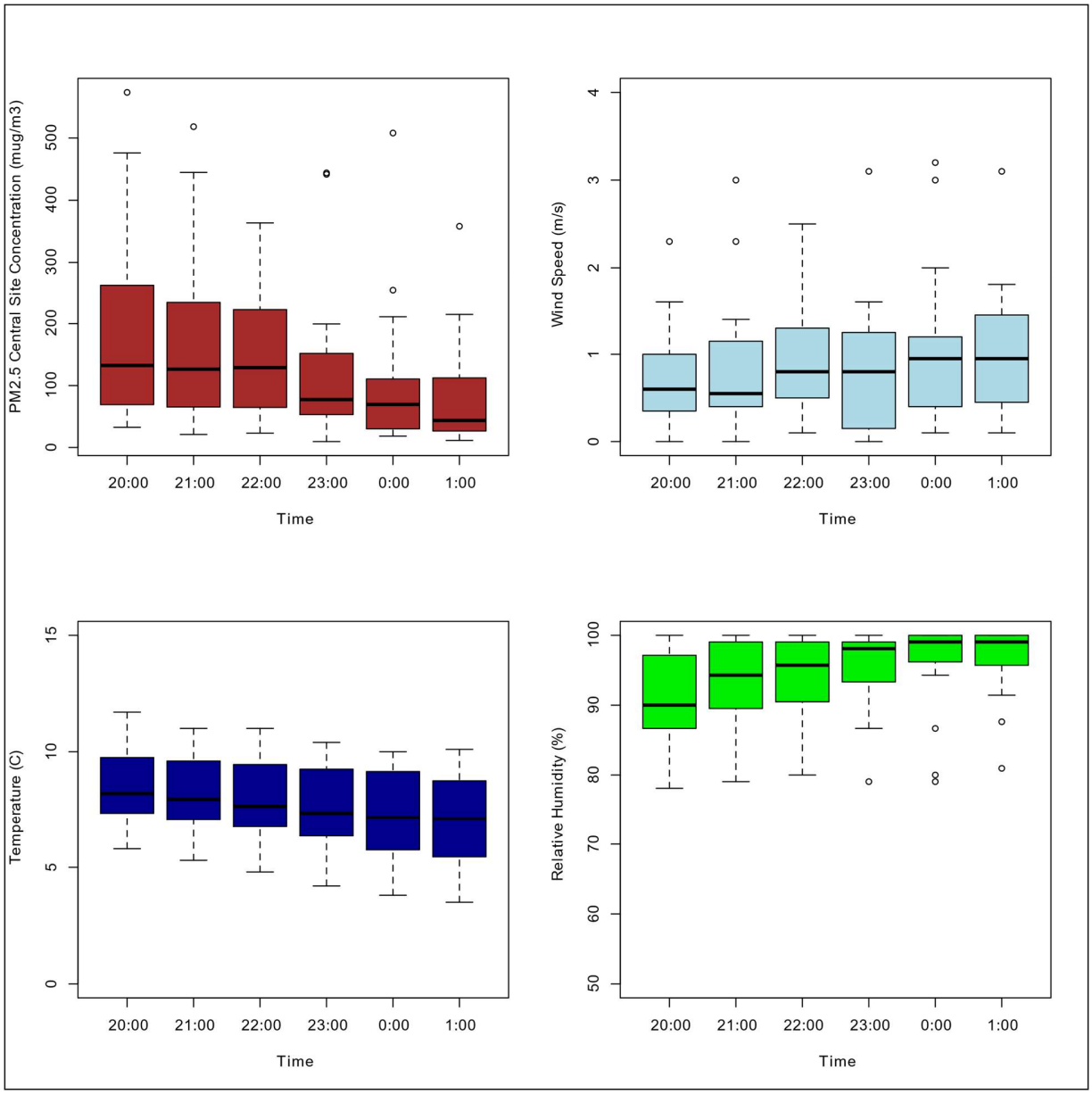

Figure S 6. Boxplots for (clockwise from upper right) wind speed, relative humidity, temperature and $PM_{2.5}$ by hour measured at the government central site for the days of mobile sampling.

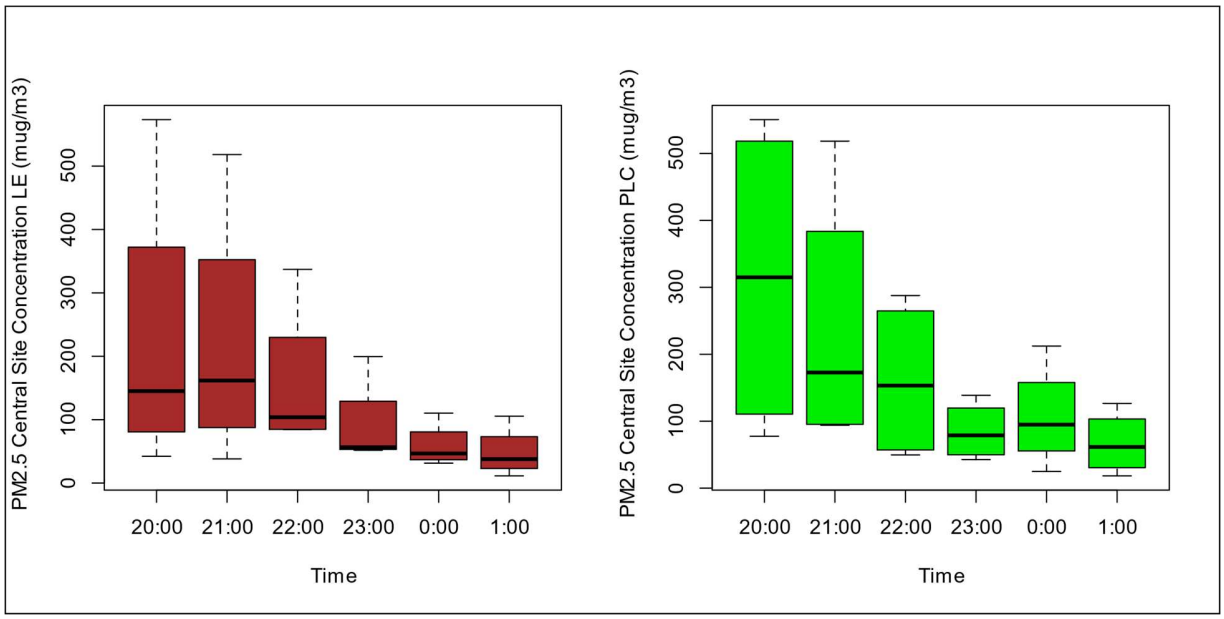

Figure S 6 cont. Boxplots for (clockwise from upper right) $PM_{2.5}$ measured at Las Encinas (central site) and Padre Las Casas government monitoring stations by hour for the days of mobile sampling at the Padre Las Casas route.

143

144

145

146

147

148

149

150

151

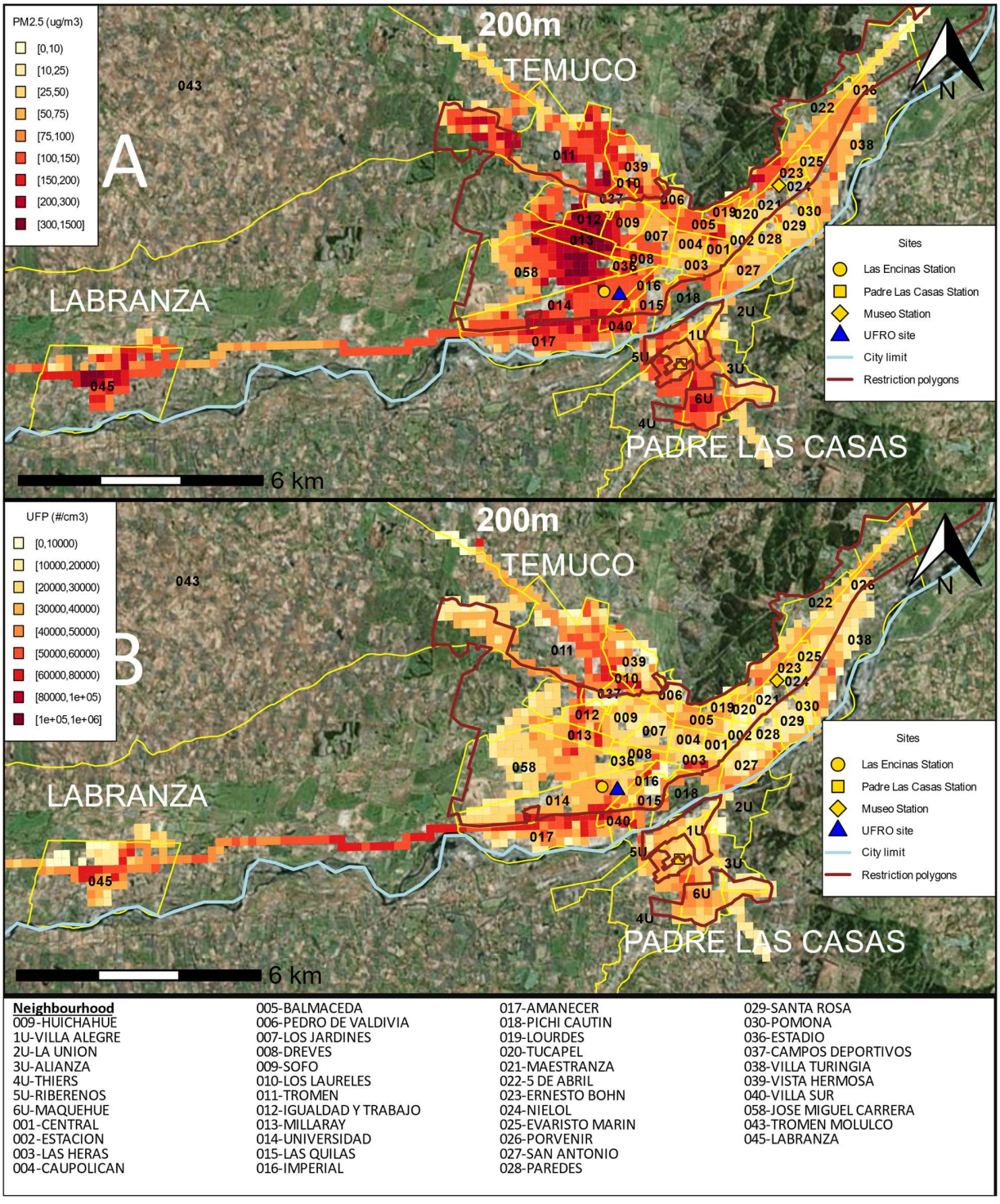

Figure S 7. Mean concentrations per cell for $PM_{2.5}$ (A) and UFP (B) at a 200-meter spatial resolution with neighborhoods indicated by number.

156

157

158

159

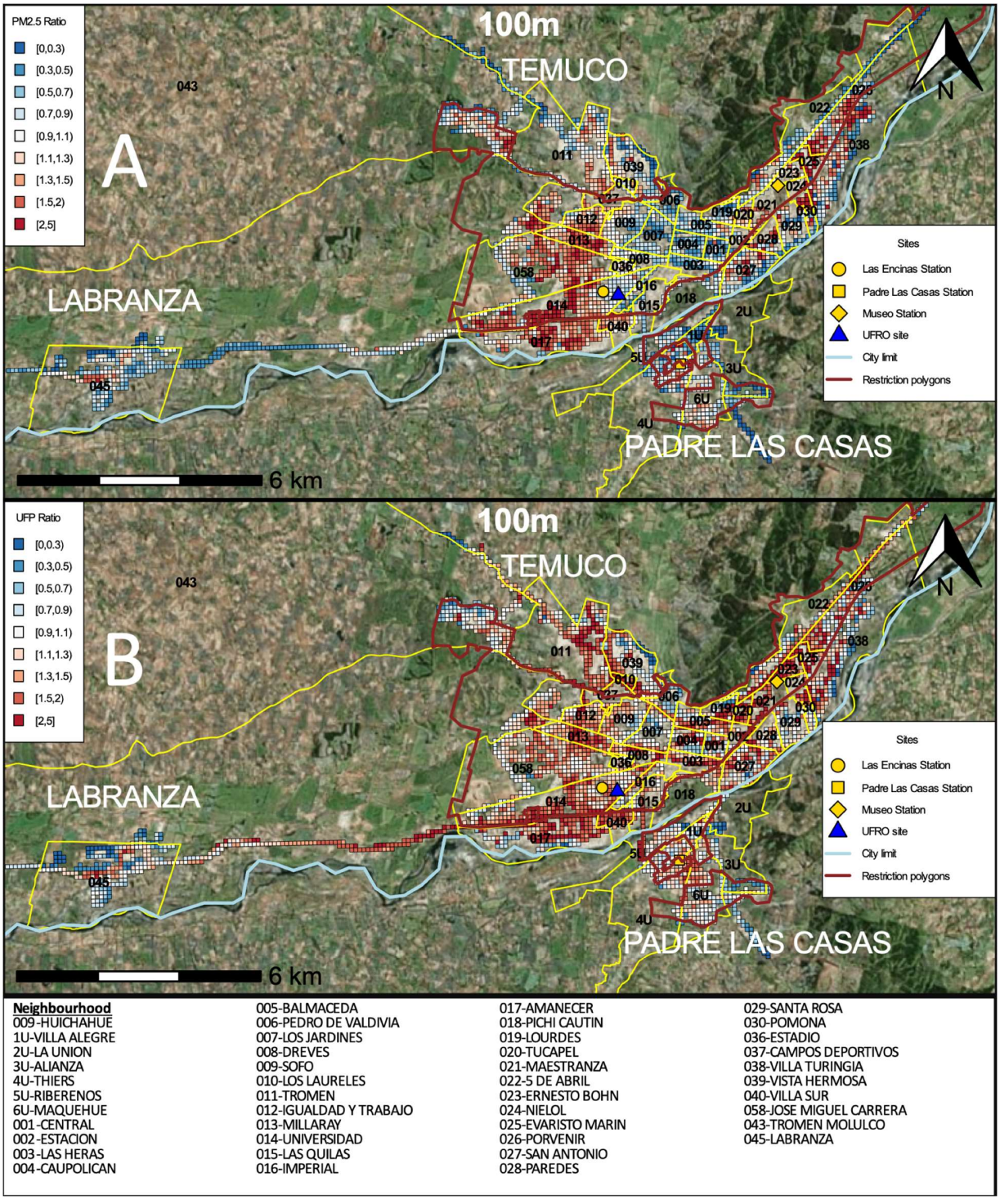

Figure S 8. Ratios of $PM_{2.5}$ (A) and UFP (B) at a 100-meter spatial resolution with neighborhoods indicated by number. Ratios above 1 are colored in orange-red tones

(darker red color indicates a higher ratio) and ratios below 1 are colored in blue tones (darker blue tone indicates lower ratio).

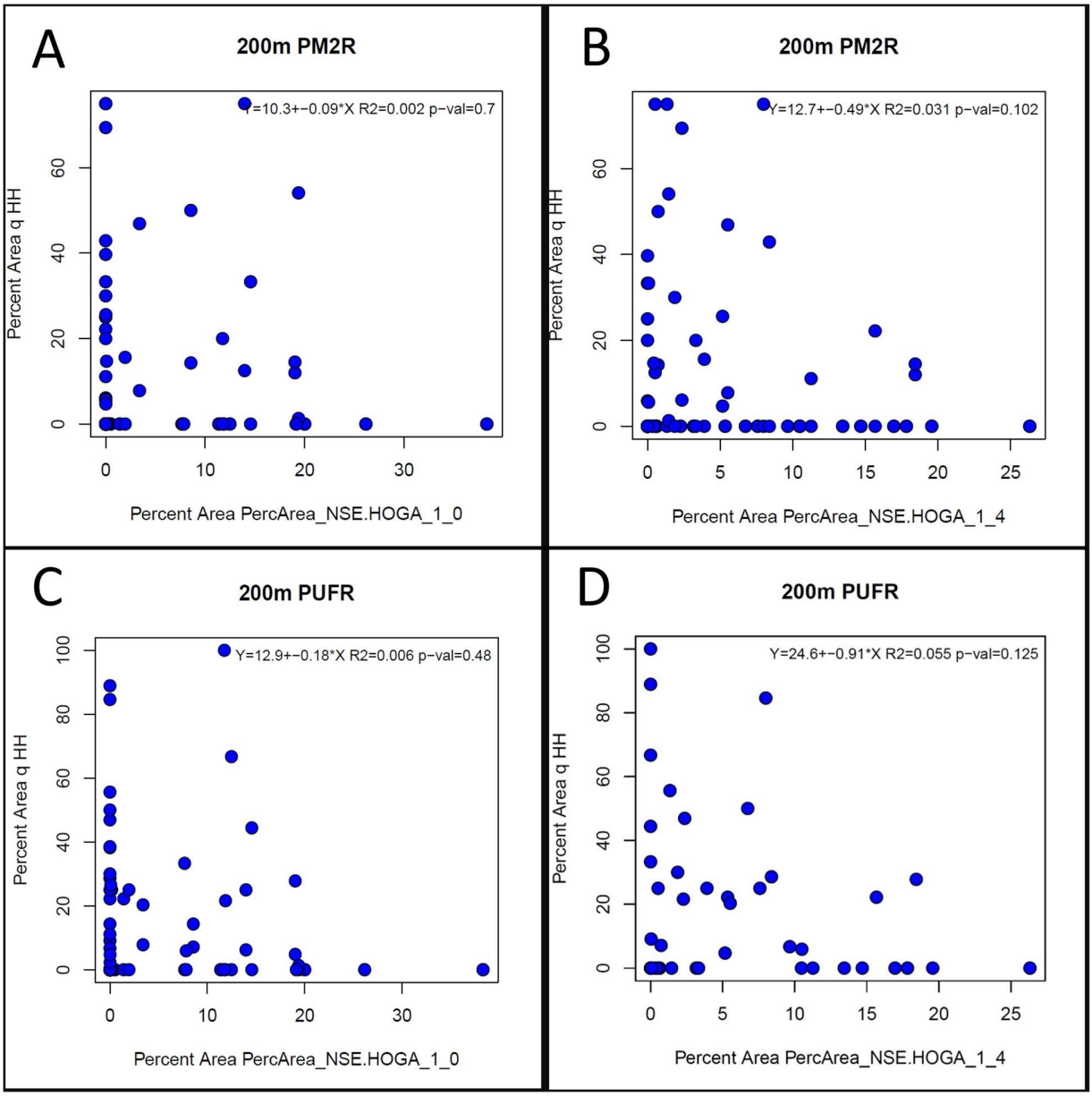

Figure S 9. Scatter plot of socioeconomic variables against presence of hotspots of $PM_{2.5}$ or UFP at a 200-meter spatial resolution. A) Percent area of homes of high purchasing power against percent area of $PM_{2.5}$ ratio hotspots, B) percent area of homes of low purchasing power against percent area of $PM_{2.5}$ ratio hotspots, C) percent area of homes of high purchasing power against percent area of UFP ratio hotspots, D) percent area of homes of low purchasing power against percent area of UFP ratio hotspots.